Supporting Information

Silver(I) coordination polymers of *trans*-5-styryl pyrimidine – from structural diversity to solid-state reactivity under sunlight

K. Mohamed Yusuf Baig[a] and Goutam Kumar Kole*[,a]

Department of Chemistry, College of Engineering and Technology, SRM Institute of Science and Technology, Kattankulathur, Tamil Nadu 603203, India.

Email: goutamks@srmist.edu.in

Table of Contents

1. Crystallographic data

Table S1. Crystallographic data for 5-Spym and **1** – **2**.

Compound	**5-Spym**	**1**	**2**
CCDC No.	2271976	2271977	2271978
Formula	$C_{12}H_{10}N_2$	$C_{12}H_{12}AgN_3O_4$	$C_{12}H_{12}AgBF_4N_2O$
Formula weight ($g.mol^{-1}$)	182.22	370.12	394.92
Temperature (K)	295(2)	295(2)	295(2)
Radiation, λ (Å)	Mo Kα (λ =0.71073)	Mo Kα (λ =0.71073)	Mo Kα (0.71073)
Crystal Colour, habit	Colorless, Block	Colorless, Block	Colorless, Block
Crystal size (mm^3)	0.330 x 0.270 x 0.240	0.192 x 0.138 x 0.118	0.270 x 0.160 x 0.110
Crystal system	Monoclinic	Monoclinic	Monoclinic
Space Group	$P2_1/c$	$P2_1/n$	$P2_1/n$
Unit cell dimensions			
a (Å)	22.3235(11)	7.799(2)	7.7806(15)
b (Å)	11.7383(5)	18.295(4)	18.880(5)
c (Å)	7.5580(4)	8.984(2)	9.480(3)
α (º)	90	90	90
β (º)	92.989(2)	93.931(14)	96.150(14)
γ (º)	90	90	90
Volume ($Å^3$)	1977.80(17)	1278.9(5)	1384.6(6)
Z	8	4	4
Calculated density ($Mg.m^{-3}$)	1.224	1.922	1.894
μ (mm^{-1})	0.074	1.593	1.499
θ range (°)	2.74 to 27.11	2.531 to 26.371	2.157 to 26.368
Reflections collected	24051	15273	27457
Independent reflections	4041	2606	2835
Parameters/ restraints	254/0	188/0	198/3
GooF on F^2	1.064	1.098	1.060
R_1 [I>2σ(I)] [a]	0.0433(3298)	0.0254(2418)	0.033(2493)
wR_2 (all data) [b]	0.1273(4041)	0.0660(2606)	0.0958(2835)
Maximum/minimum residual electron density ($e.Å^{-3}$)	0.143/-0.129	0.383/-0.377	0.764/-0.512

Table S2. Crystallographic data for **3** – **5**.

Compound	**3**	**4**	**5**
CCDC No.	2271981	2271979	2271980
Formula	$C_{12}H_{10}AgF_6N_2Sb$	$C_{13}H_{10}AgF_3N_2O_3S$	$C_{14}H_{10}AgF_3N_2O_2$
Formula weight ($g.mol^{-1}$)	525.85	439.16	403.11
Temperature (K)	295(2)	295(2)	295(2)
Radiation, λ (Å)	Mo Kα (0.71073)	Mo Kα (0.71073)	Mo Kα (0.71073)
Crystal Colour, habit	Colorless, Needle	Colorless, Block	Colorless, Block
Crystal size (mm^3)	0.240 x 0.083 x 0.072	0.290 x 0.200 x 0.140	0.180 x 0.150 x 0.120
Crystal system	Orthorhombic	Monoclinic	Monoclinic
Space Group	*Pnma*	$P2_1/c$	$C2/c$
Unit cell dimensions			
a (Å)	12.102(4)	6.6106(9)	36.304(10)
b (Å)	6.6333(11)	17.709(2)	5.3887(9)
c (Å)	17.915(4)	12.3217(17)	15.575(4)
α (º)	90	90	90
β (º)	90	94.626(4)	110.695(16)
γ (º)	90	90	90
Volume ($Å^3$)	1438.2(6)	1437.8(3)	2850.4(12)
Z	4	4	8
Calculated density ($Mg.m^{-3}$)	2.429	2.029	1.879
μ (mm^{-1})	3.302	1.597	1.455
θ range (°)	2.031 to 26.370	2.018 to 26.370	2.624 to 26.371
Reflections collected	23119	26235	17957
Independent reflections	1603	2938	2911
Parameters/ restraints	185/197	264/120	247/120
GooF on F^2	1.123	1.106	1.056
R_1 [I>2σ(I)] [a]	0.0197(1499)	0.0303(2657)	0.0262(2670)
wR_2 (all data) [b]	0.0509(1603)	0.0742(2938)	0.0686(2911)
Maximum/minimum residual electron density ($e.Å^{-3}$)	0.378/-0.685	0.493/- 0.451	0.452/-0.800

2. Additional crystallographic diagrams

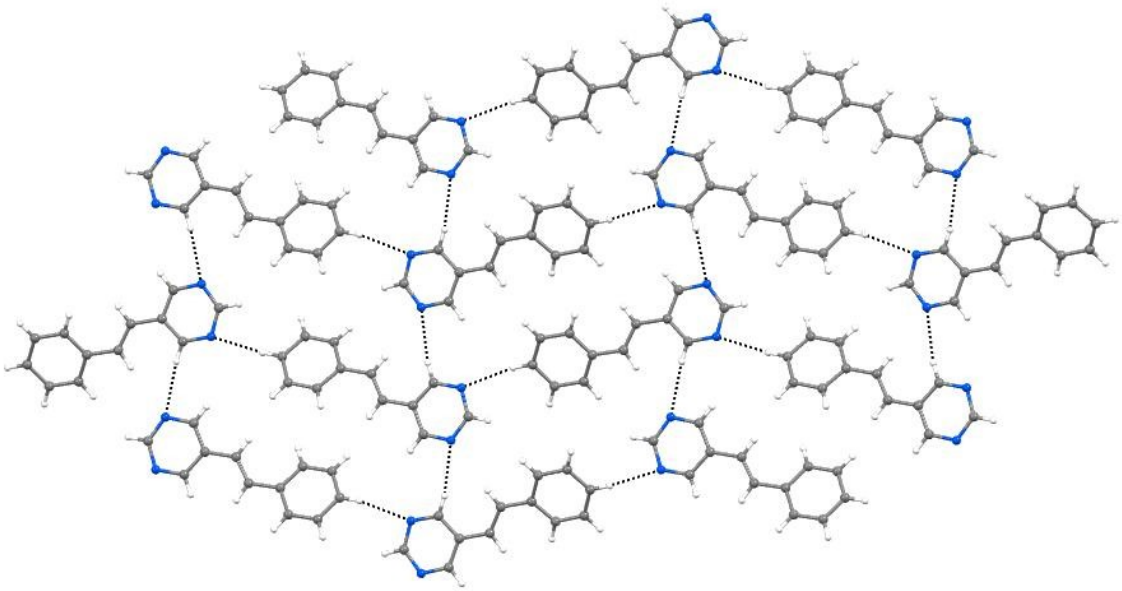

Fig. S1: Crystal packing of 5-Spym showing C−H···N weak interactions, viewed approximately along *c*-direction.

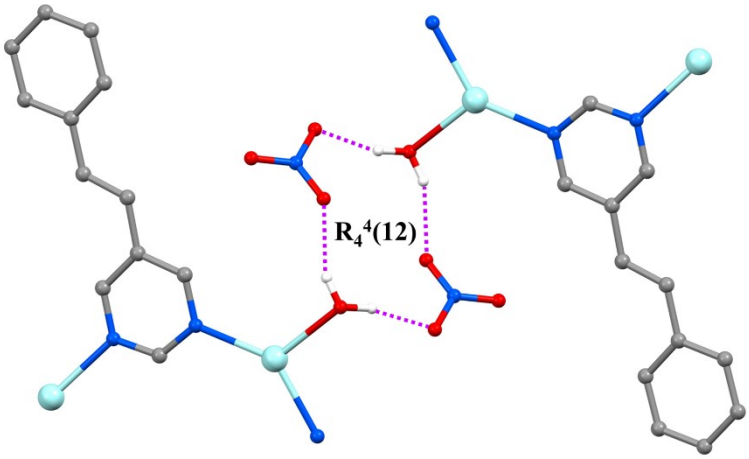

Fig. S2. Hydrogen bonding interaction between nitrate anion and aqua ligands from neighbouring chains and the formation of 12-membered ring of graph set $\mathbf{R}_4^4(12)$ in **1**.

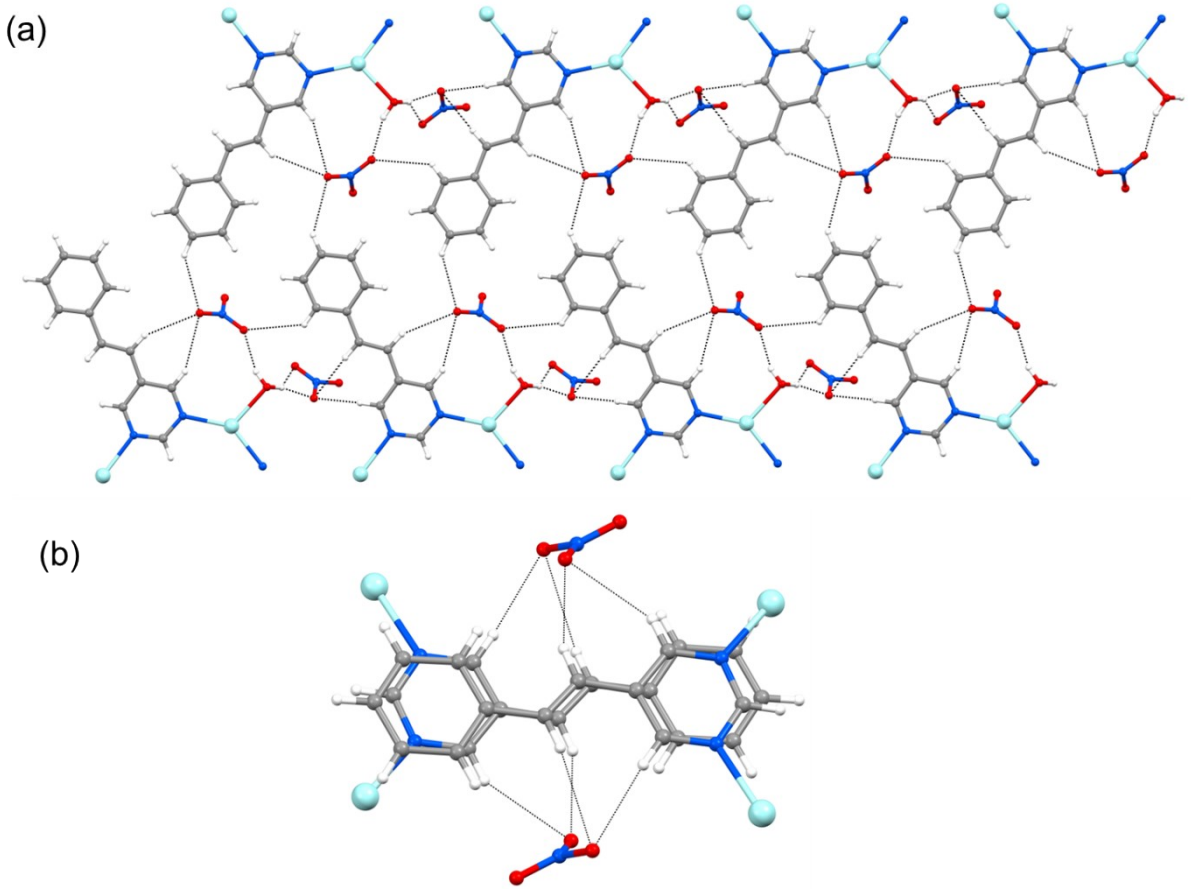

Fig. S3: (a) O−H···O hydrogen bonding and weak C−H···O interaction played by the nitrate anion, and (b) C−H···O weak interaction of nitrate anion with two stacked 5-Spym ligands from different polymeric chains.

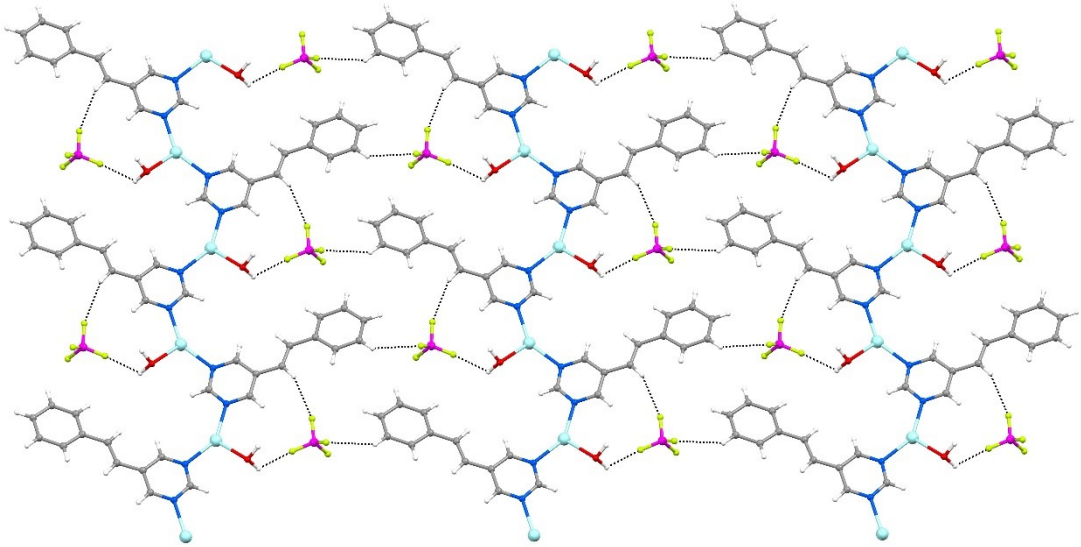

Fig. S4: (a) O−H···F hydrogen bonding and weak C−H···F interaction played by BF_4^- anion in **2**, viewed along *a*-direction.

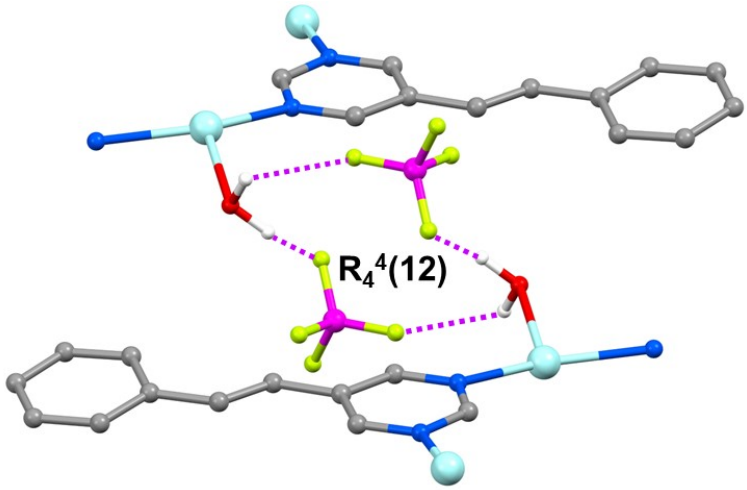

Fig. S5: Hydrogen bonding interaction between BF_4^- anion and aqua ligands from neighbouring chains and the formation of 12-membered ring of graph set $\mathbf{R}_4^4(12)$ in **2**.

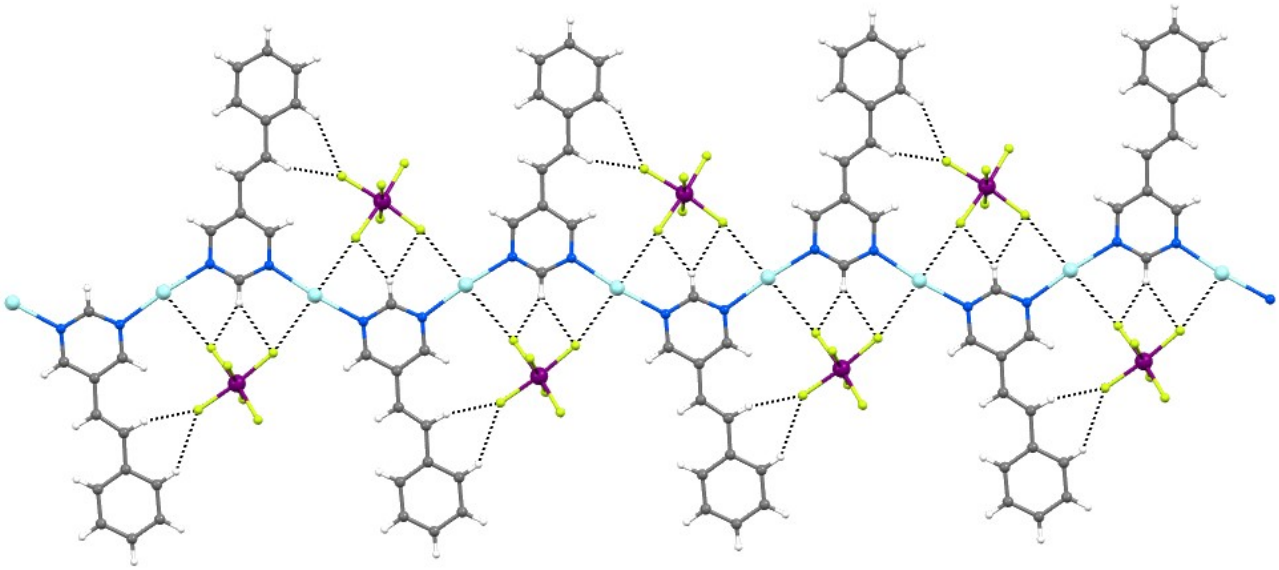

Fig. S6: C–H···F and Ag···F weak interaction played by SbF_6^- anion in **3**, viewed along *a*-direction.

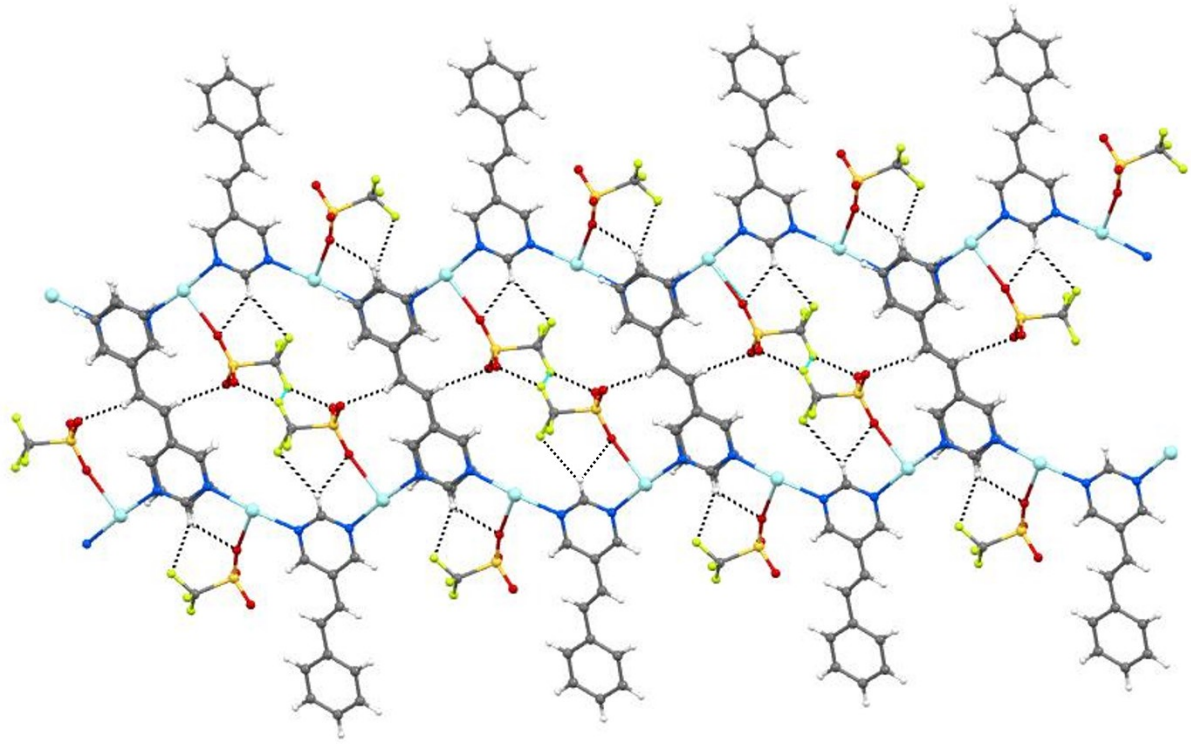

Fig. S7: Various weak interactions played by $CF_3SO_3^-$ anion in **4**, viewed along *a*-direction.

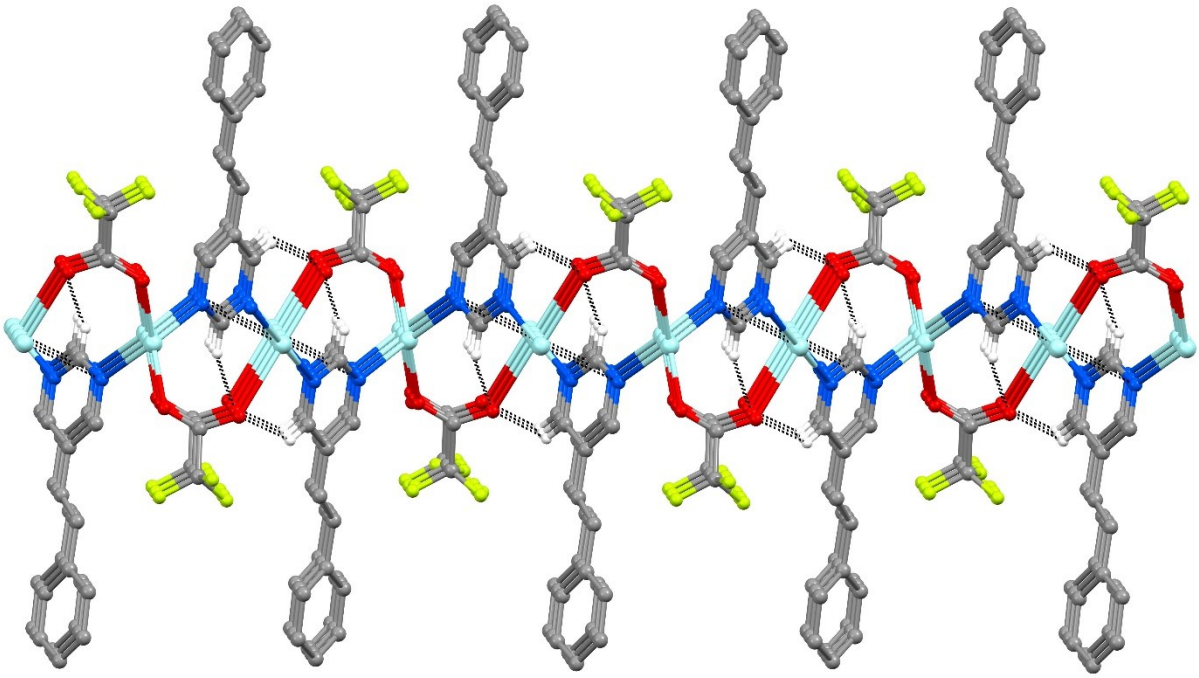

Fig. S8: Two-dimensional network of **5** is viewed approx. along *b*-axis. C−H···O and Ag(I)···N interactions can be observed.

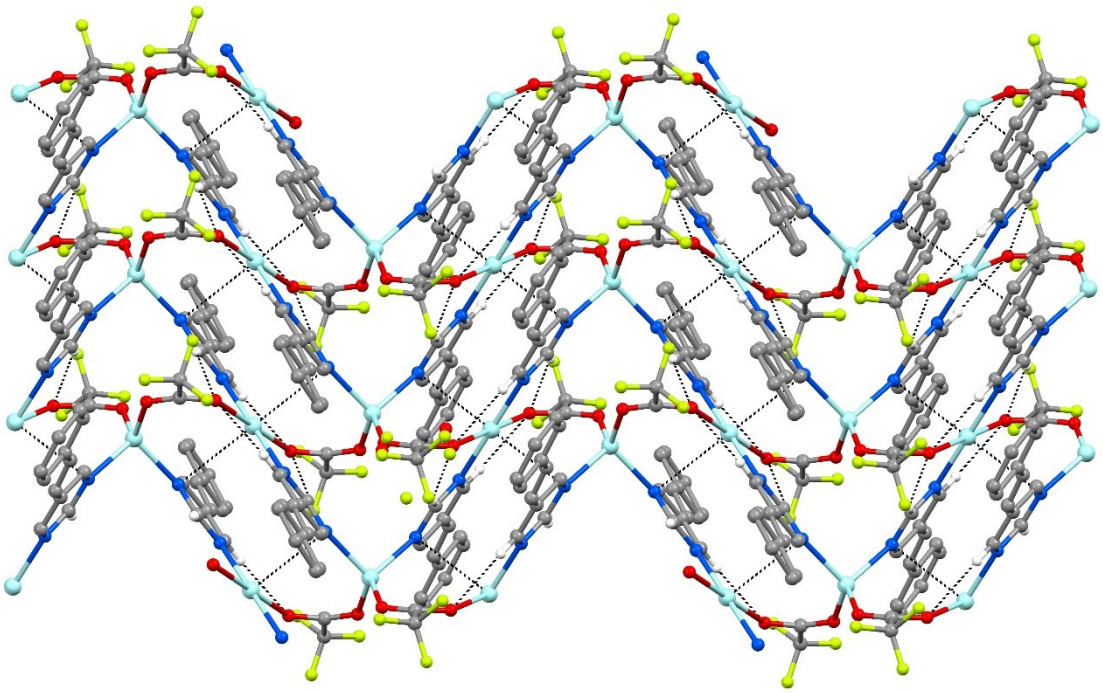

Fig. S9: Another view of two-dimensional network of 5 shows C−H···O and Ag(I)···N interactions present in **5**.

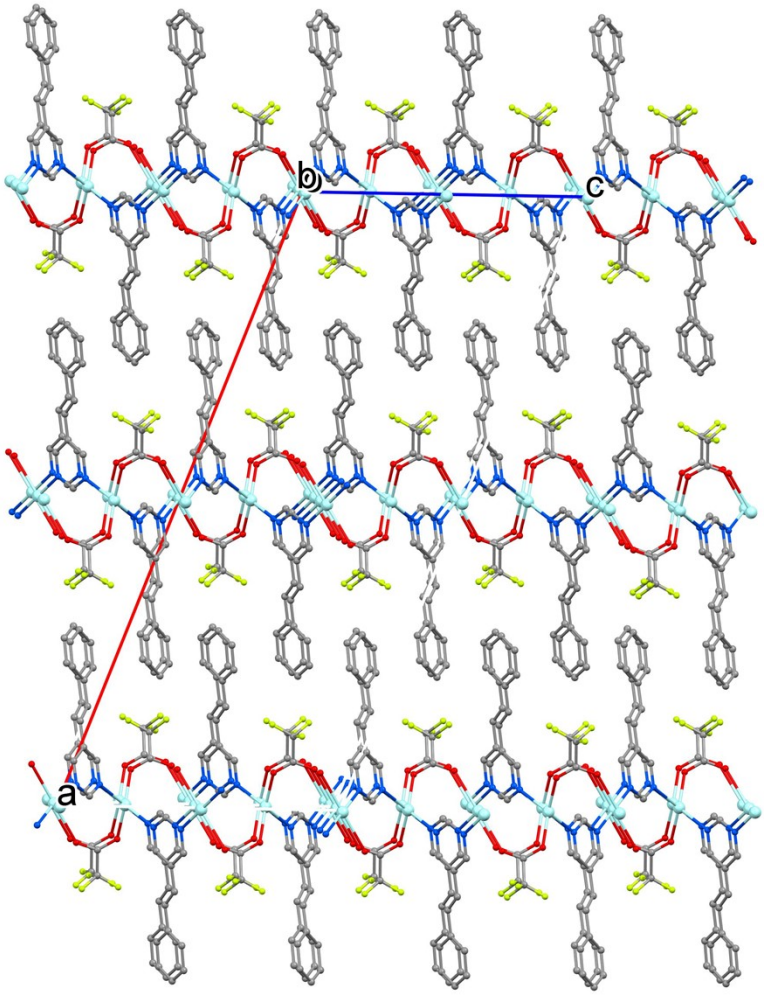

Fig. S10: Interdigitation of two-dimensional sheets of **5**, viewed along *b*-direction.

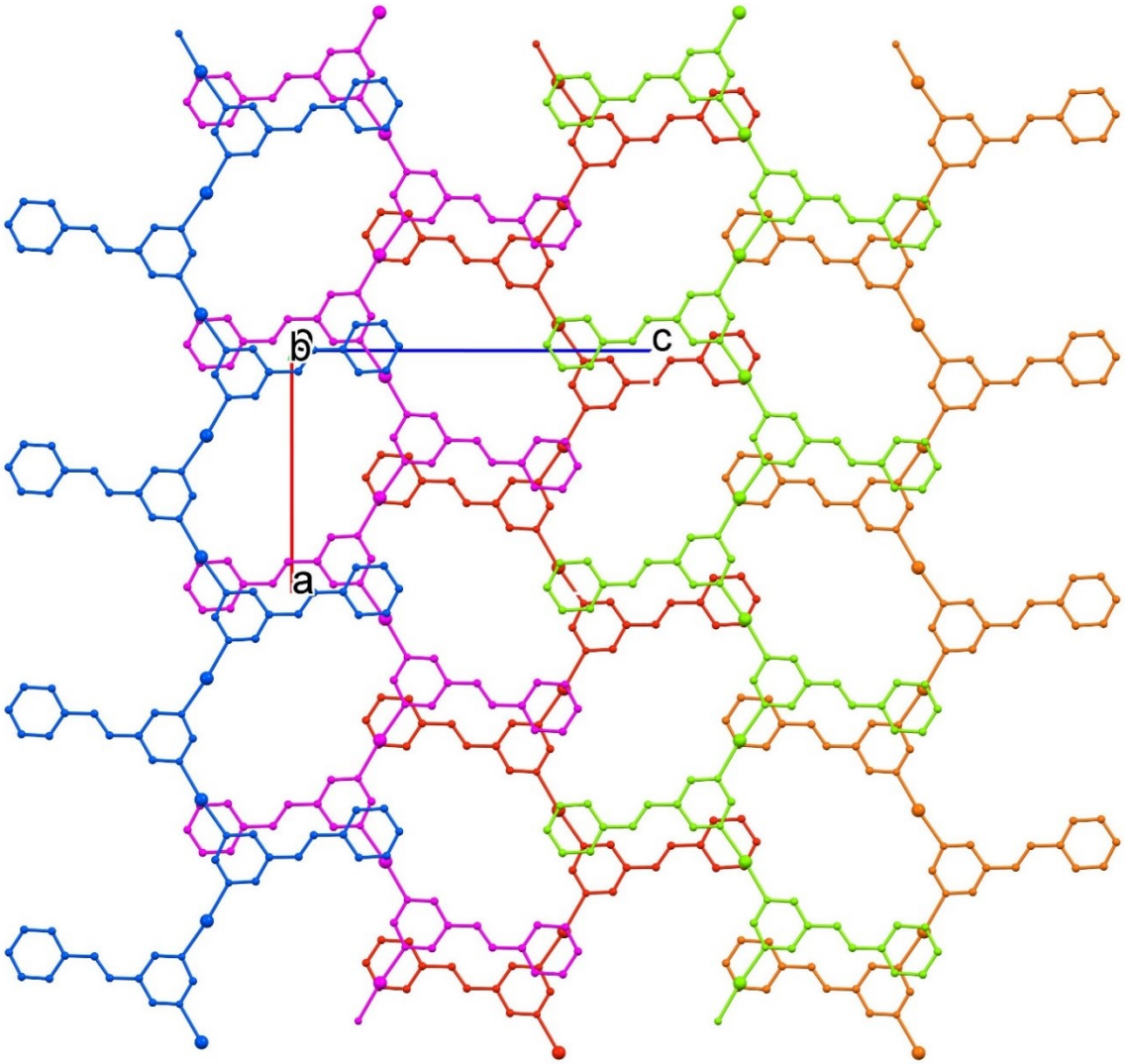

Fig. S11: Five parallel zigzag chains of 3 are shown in different colours. The chains propagate along a-direction. Chain growth due to photodimerization is expected to propagate along *b*-direction (infinitely parallel stacking). Also stacking of 5-Spym happens between two different chains of both the sides (left and right). So, the chain growth will also propagate along c-direction. Therefore, the photodimerized products is expected to have a three-dimensional network. Anions are not shown for clarity.

3. ^{1}H NMR Spectra

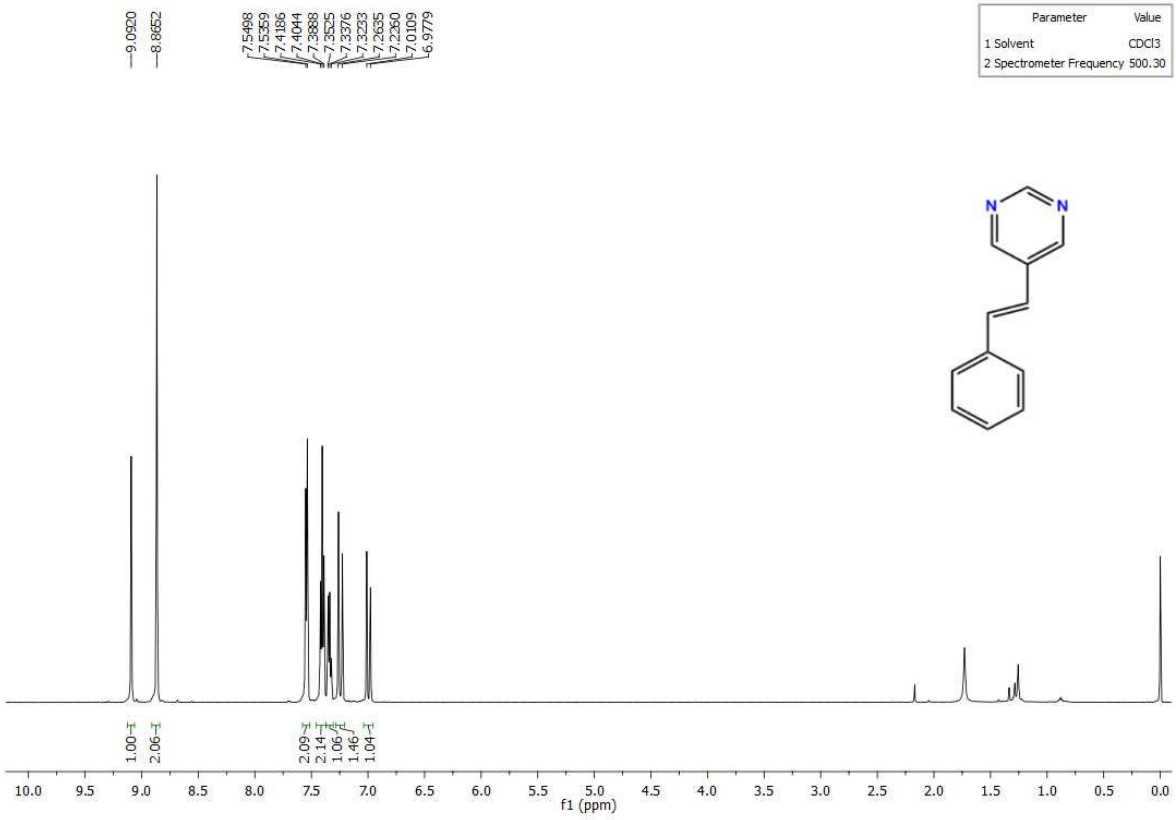

Fig. S12: ^{1}H NMR (500 MHz, $CDCl_3$) spectrum of *trans*-5-Spym ligand.

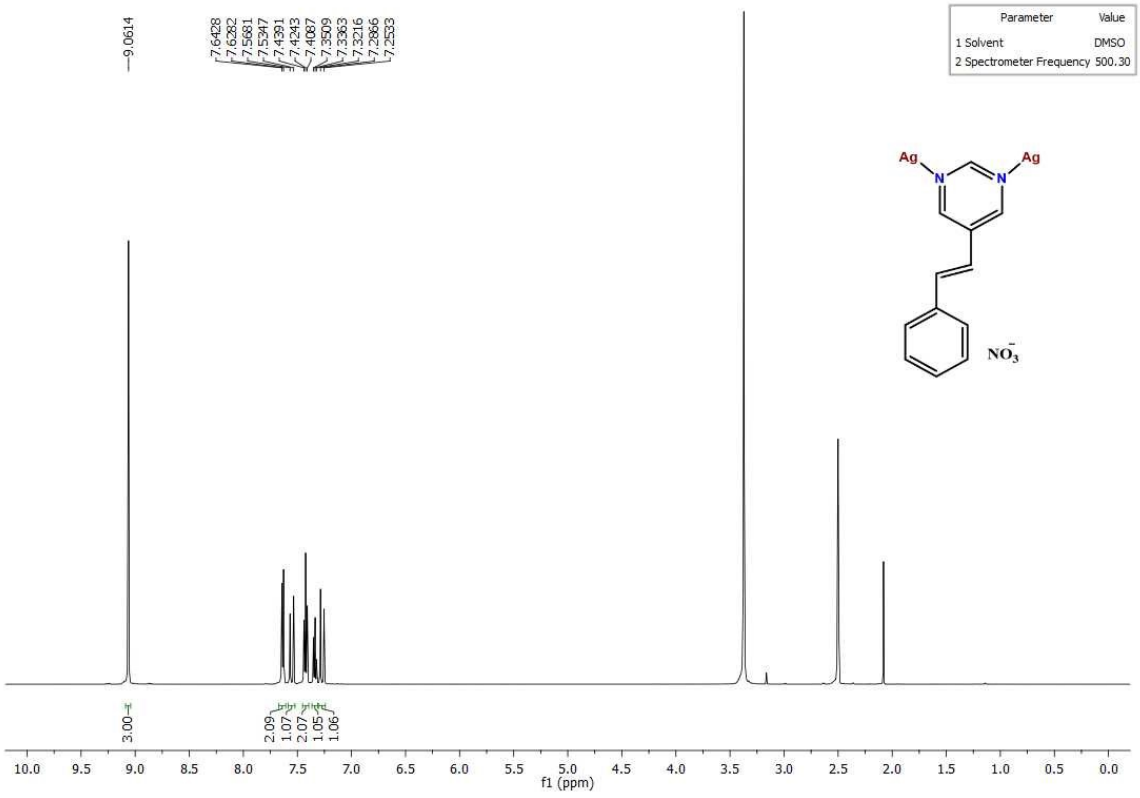

Fig. S13: ^{1}H NMR (500 MHz, DMSO-d_6) spectrum of **1** before irradiation under sunlight.

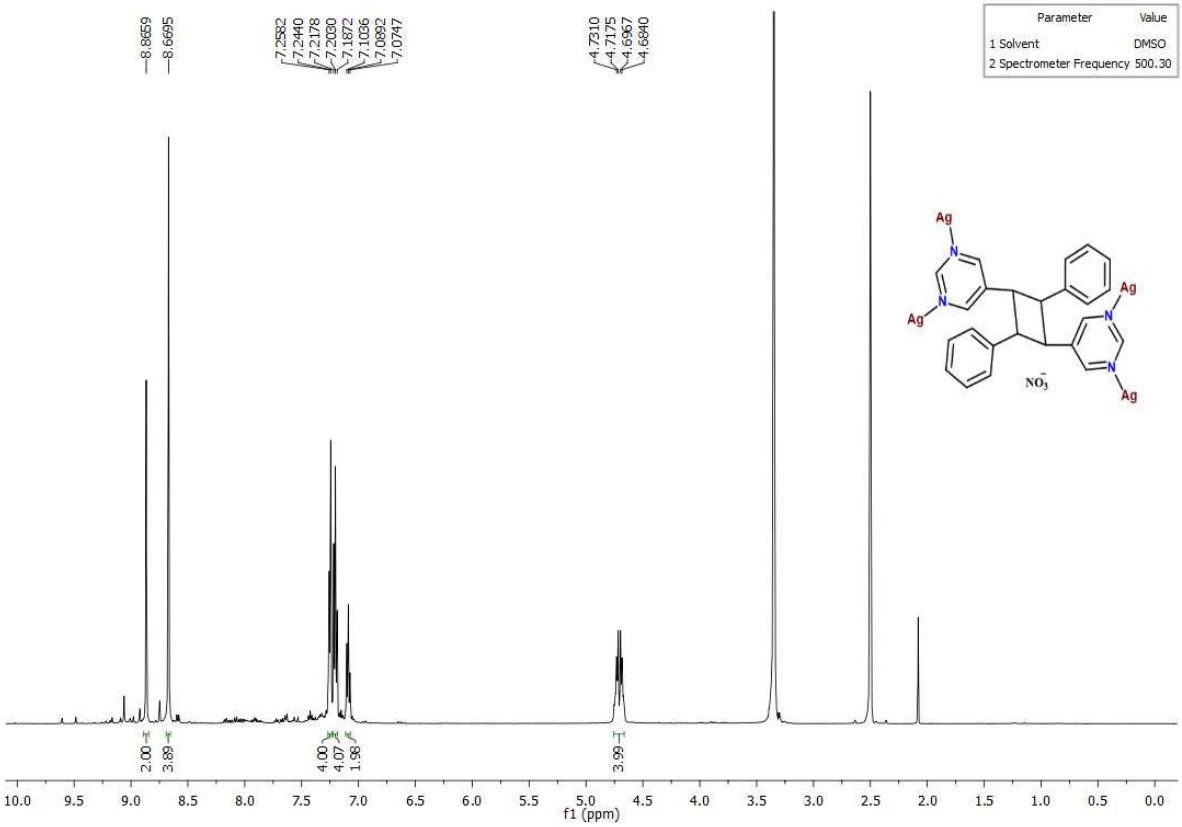

Fig. S14: ^{1}H NMR (500 MHz, DMSO-d_6) spectrum of **1** after irradiation under sunlight.

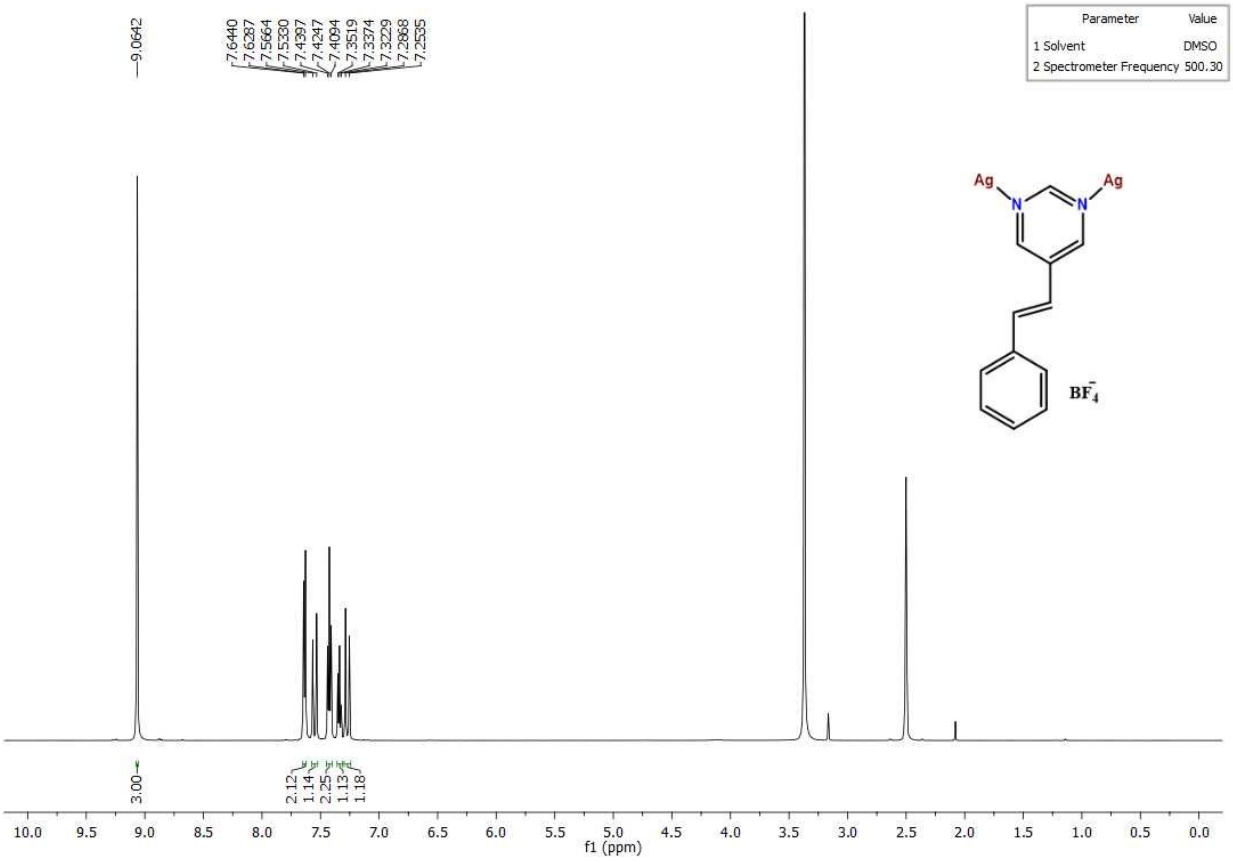

Fig. S15: ^{1}H NMR (500 MHz, DMSO-d_6) spectrum of **2** before irradiation under sunlight.

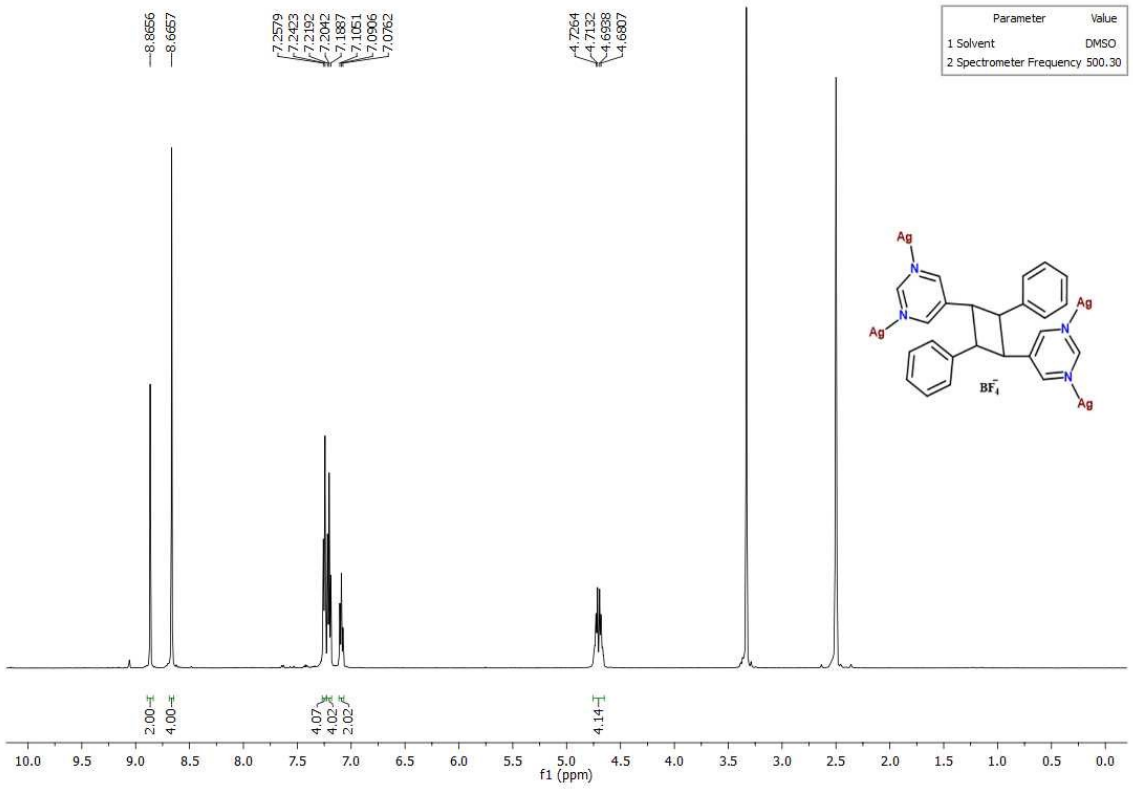

Fig. S16: ^{1}H NMR (500 MHz, DMSO-d_6) spectrum of **2** after irradiation under the sunlight.

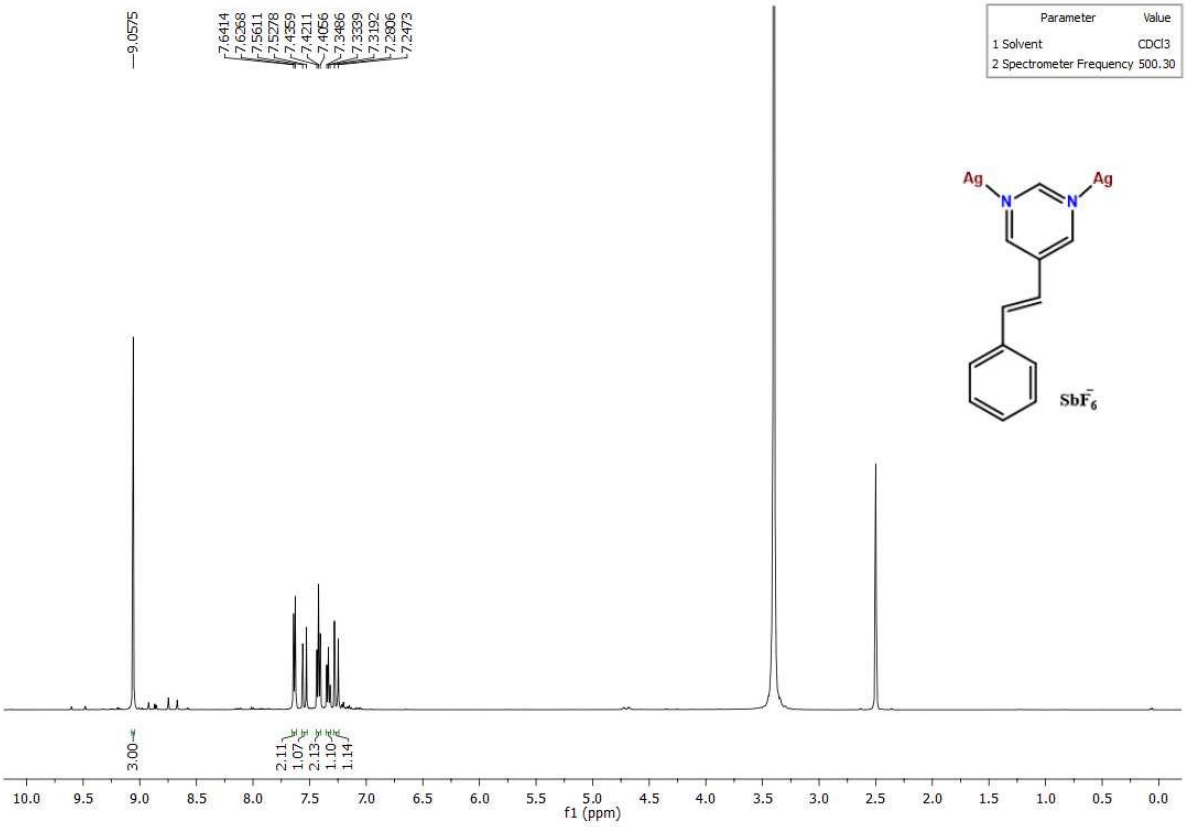

Fig. S17: ^{1}H NMR (500 MHz, DMSO-d_6) spectrum of **3** before irradiation under sunlight.

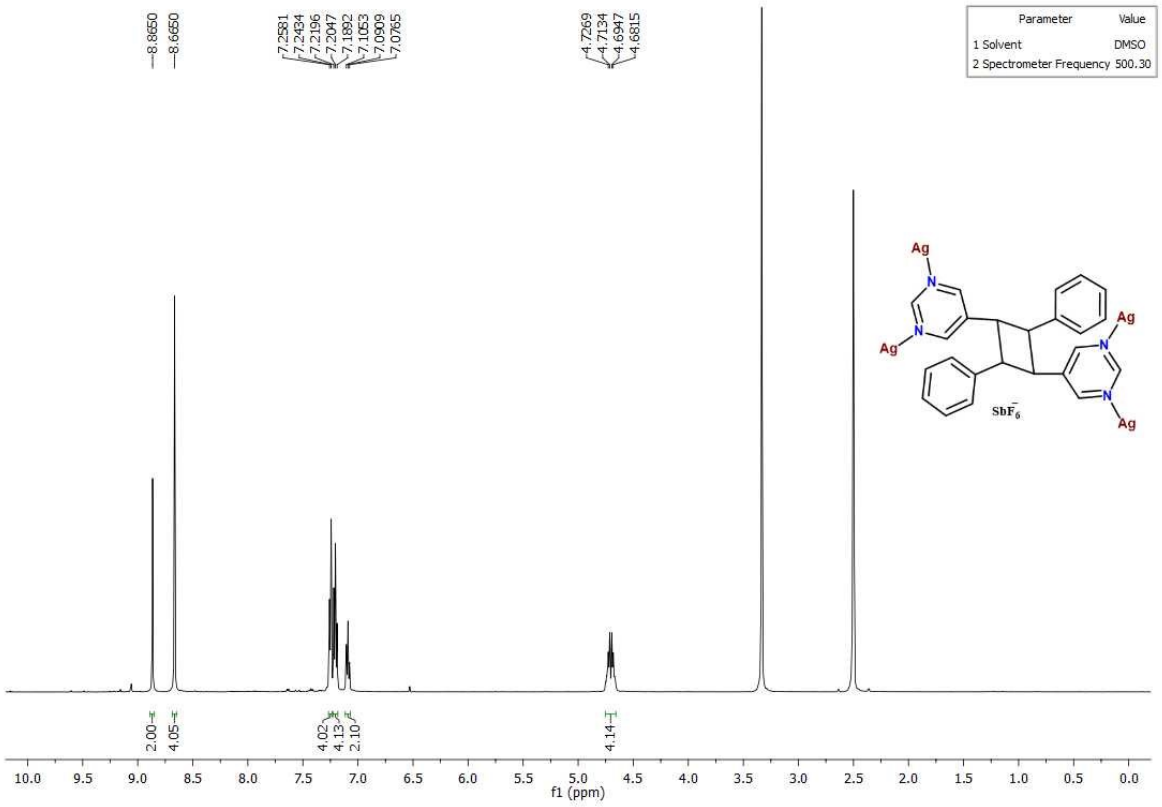

Fig. S18: ^{1}H NMR (500 MHz, DMSO-d_6) spectrum of **3** after irradiation under the sunlight.

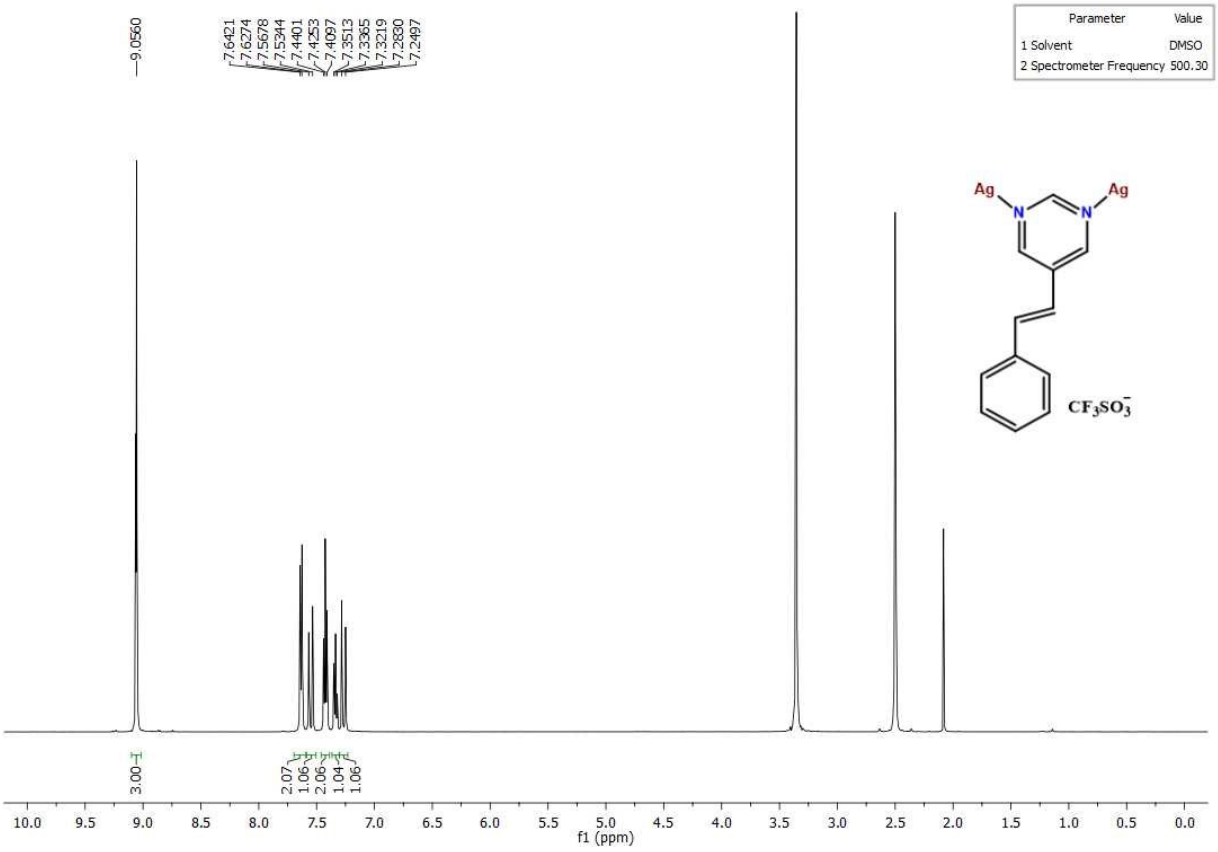

Fig. S19: ^{1}H NMR (500 MHz, DMSO-d_6) spectrum of **4** before irradiation under sunlight.

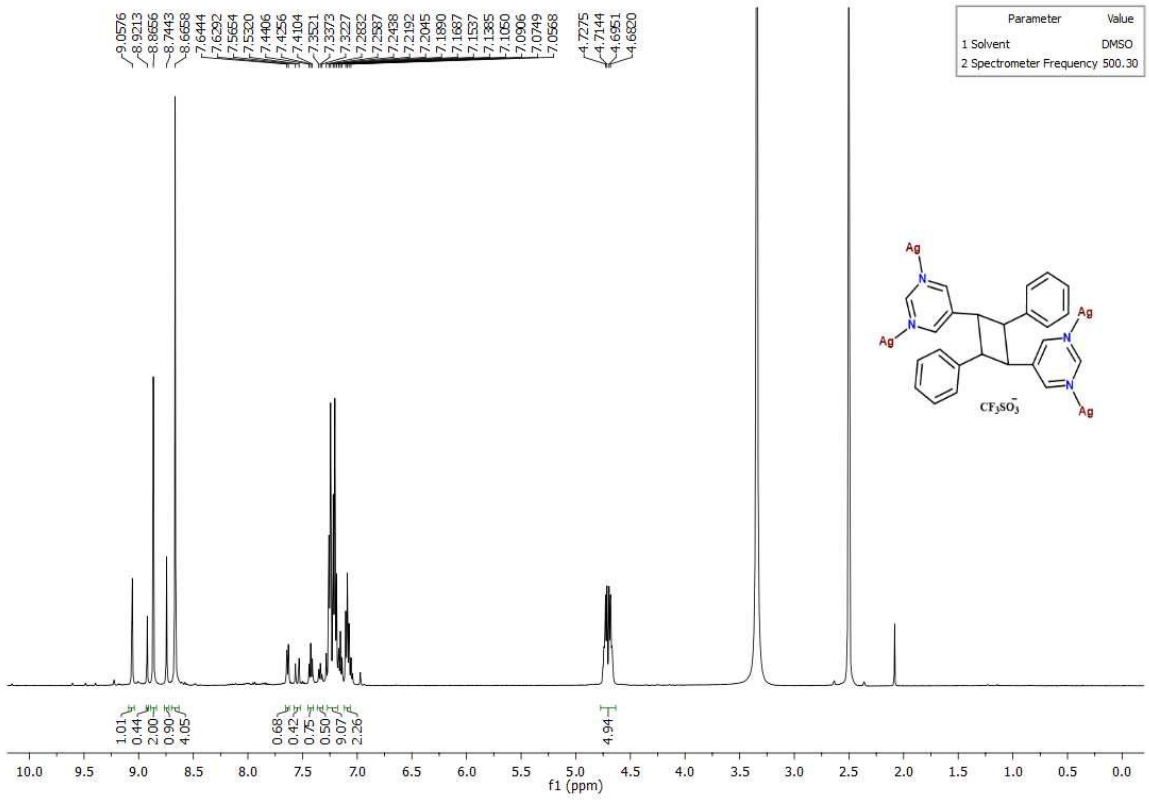

Fig. S20: ^{1}H NMR (500 MHz, DMSO-d_6) spectrum of **4** after irradiation under the sunlight.

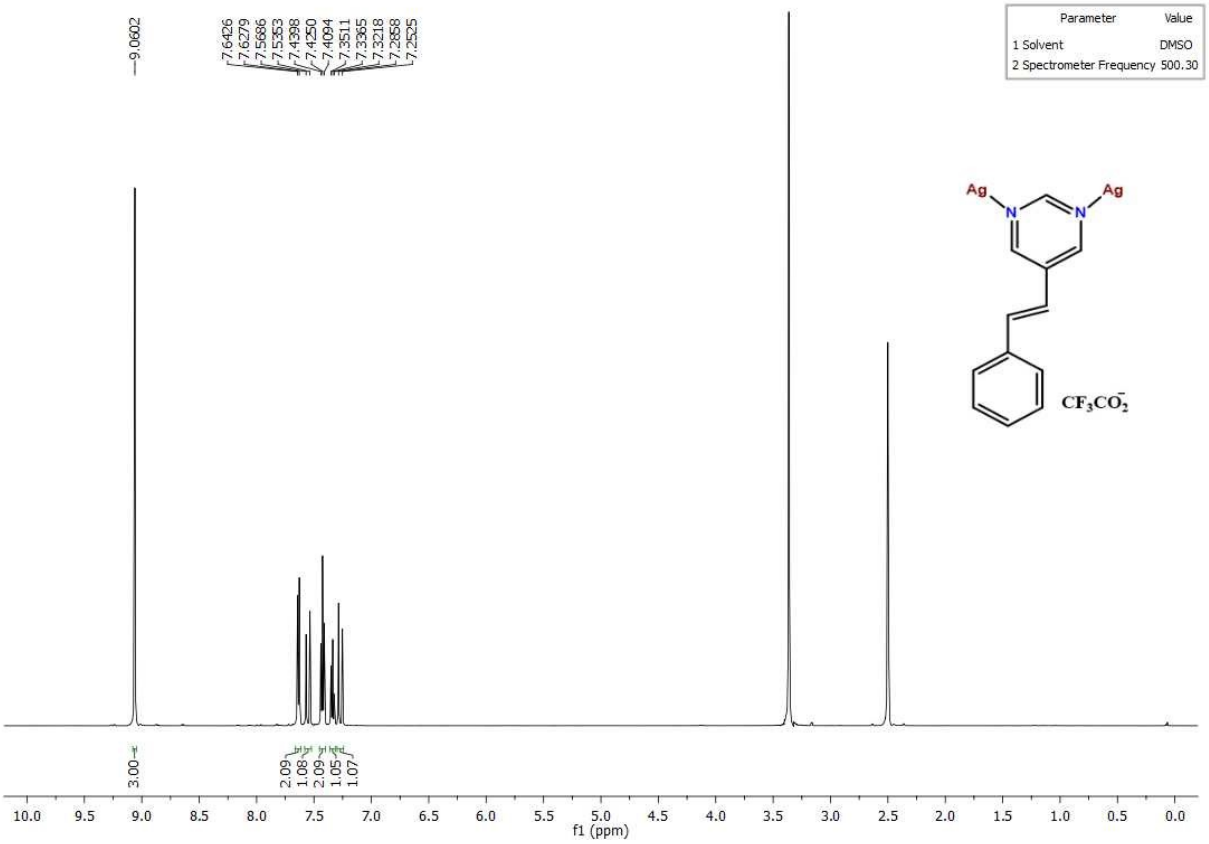

Fig. S21: ^{1}H NMR (500 MHz, DMSO-d_6) spectrum of **5** before irradiation under sunlight.

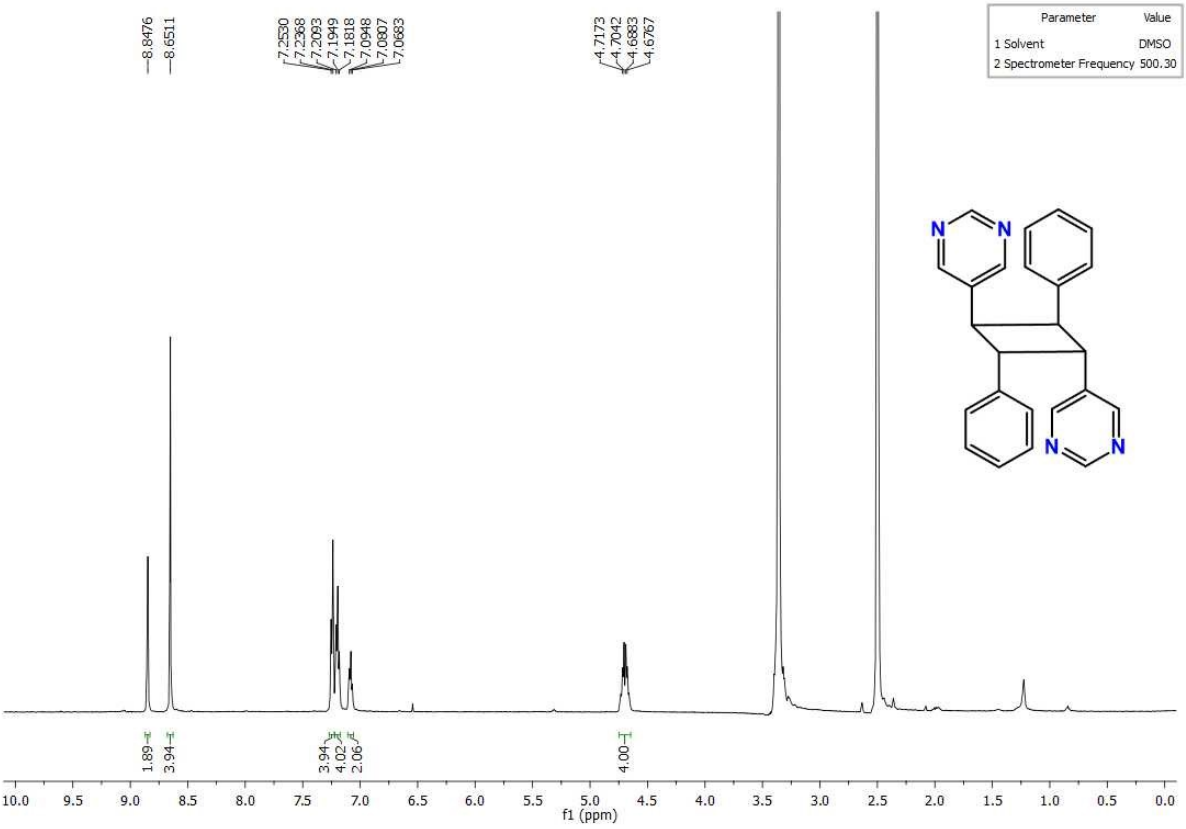

Fig. S22: ^{1}H NMR (500 MHz, DMSO-d_6) spectrum of isolated ***rctt*-bpcb.**

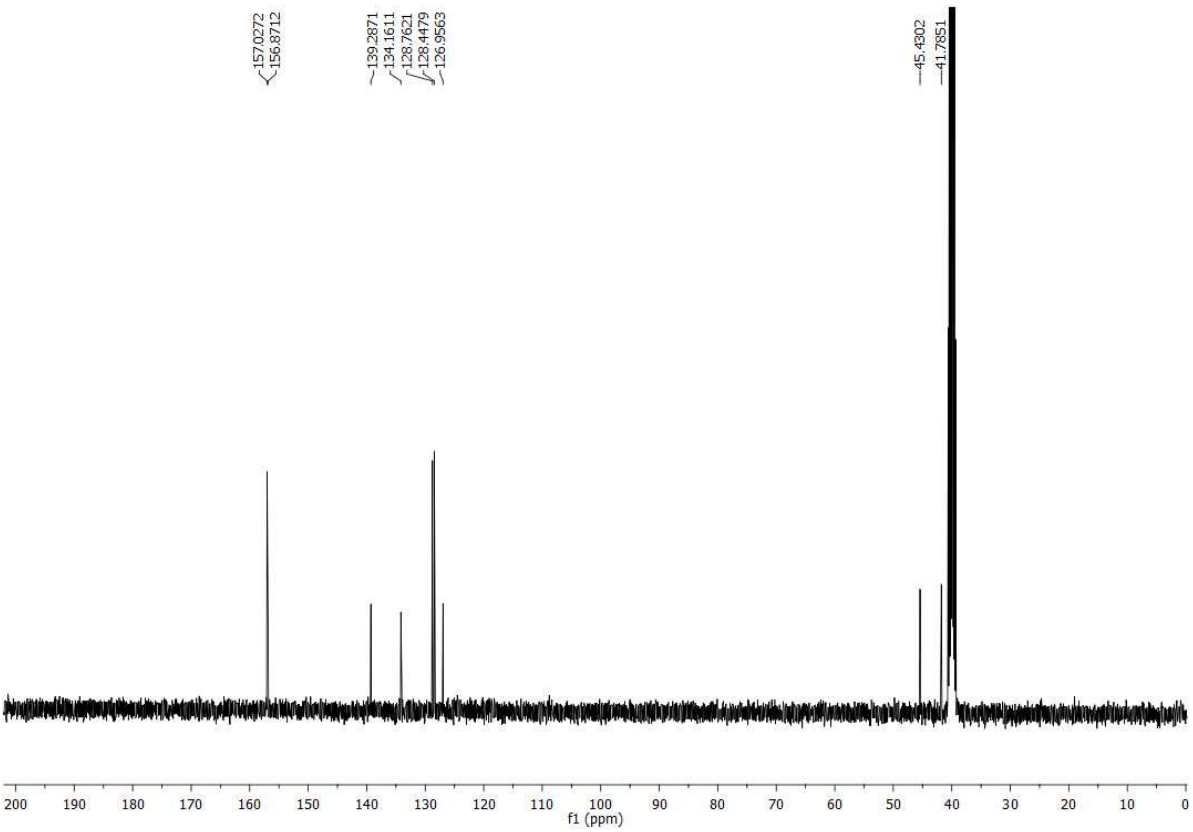

Fig. S23: ^{13}C NMR (101 MHz, DMSO-d_6) spectrum of isolated ***rctt*-bpcb.**

4. FT-IR Spectra

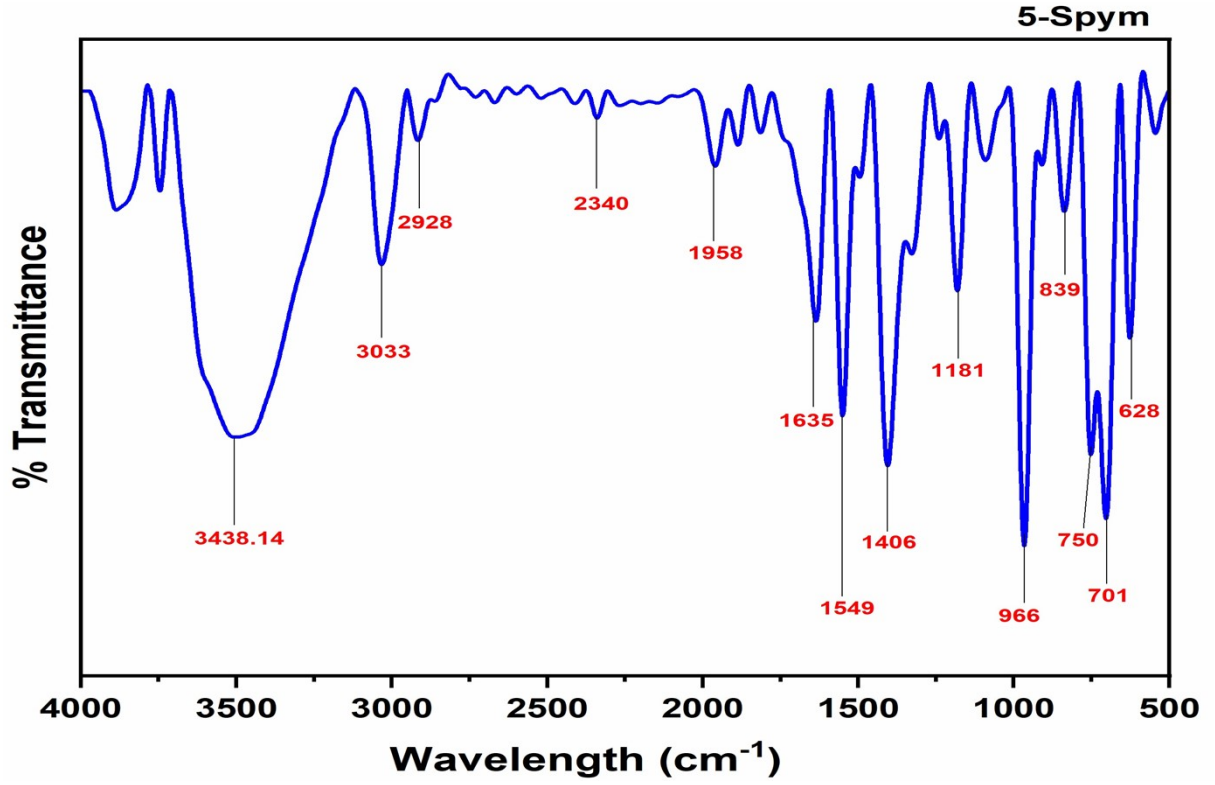

Fig. S24: FT-IR (KBr, cm^{-1}) spectrum of 5-Spym.

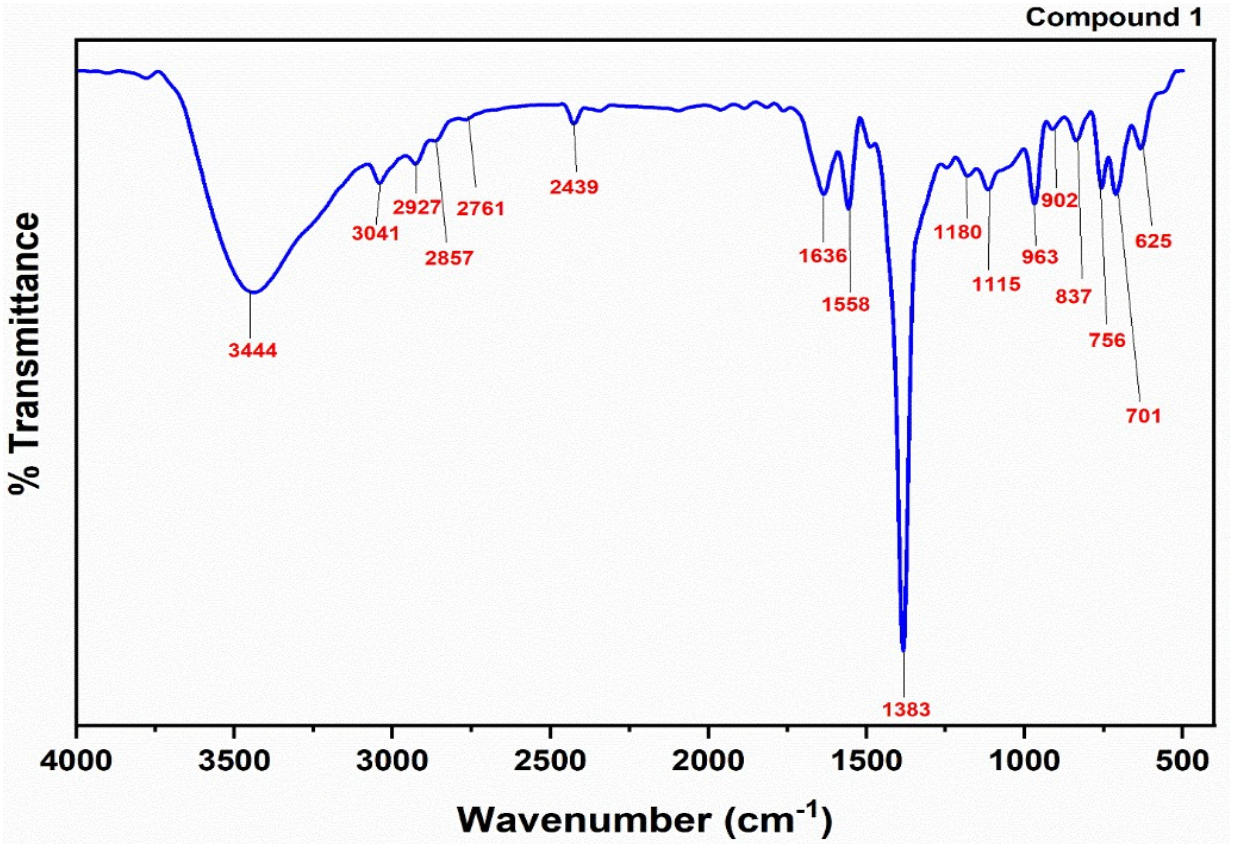

Fig. S25: FT-IR (KBr, cm^{-1}) spectrum of **1**.

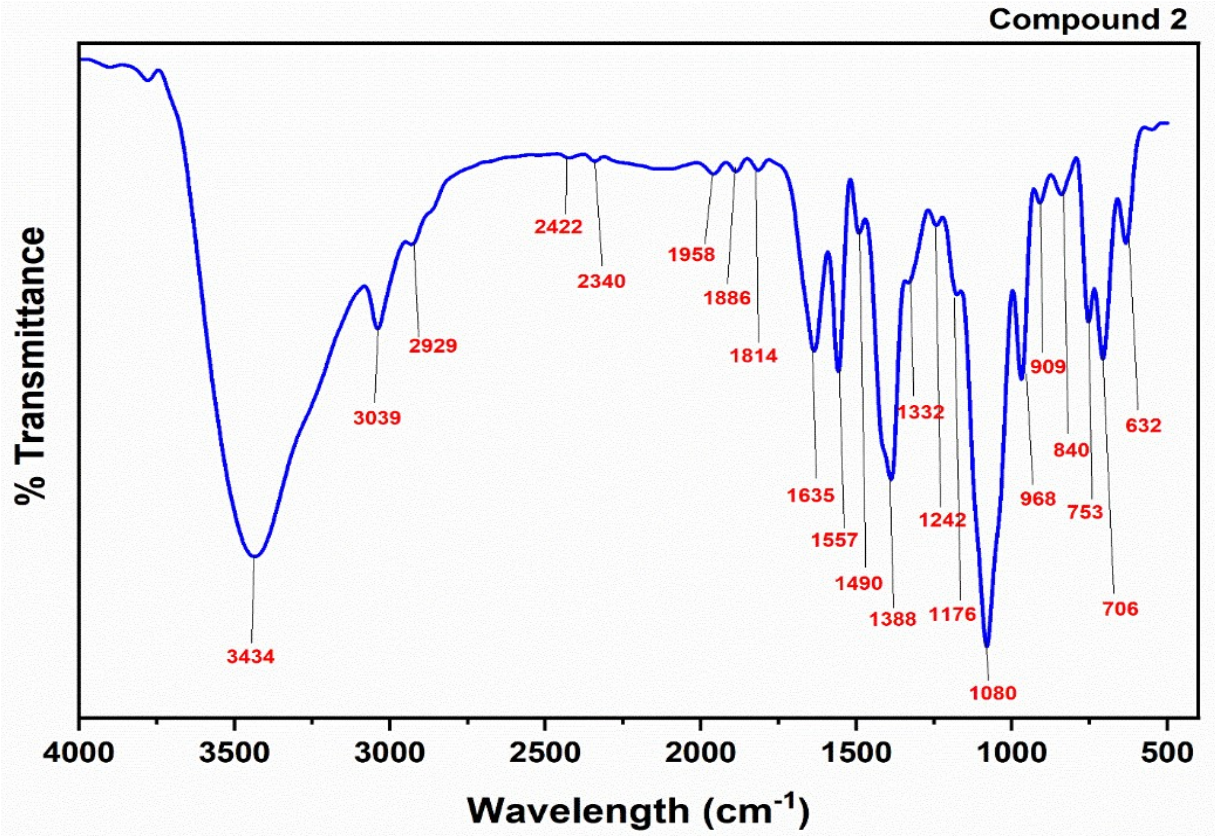

Fig. S26: FT-IR (KBr, cm^{-1}) spectrum of **2**.

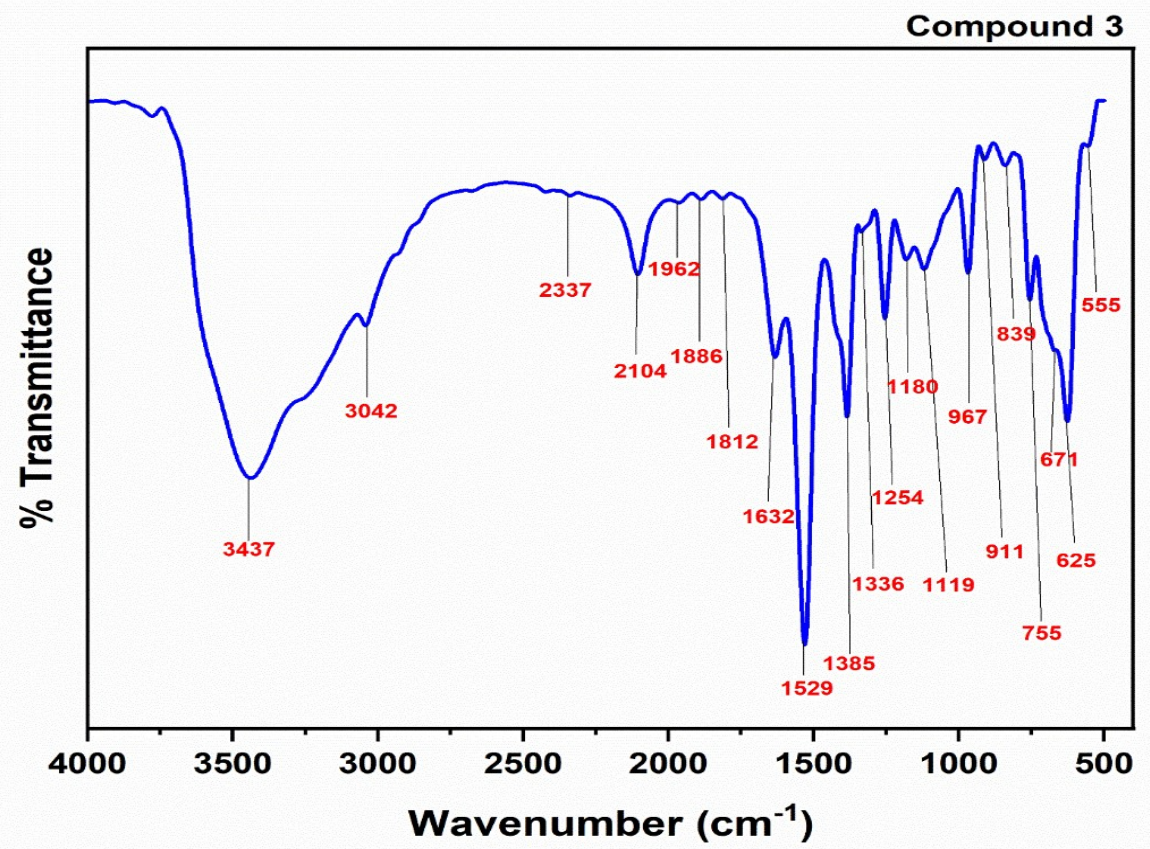

Fig. S27: FT-IR (KBr, cm^{-1}) spectrum of **3**.

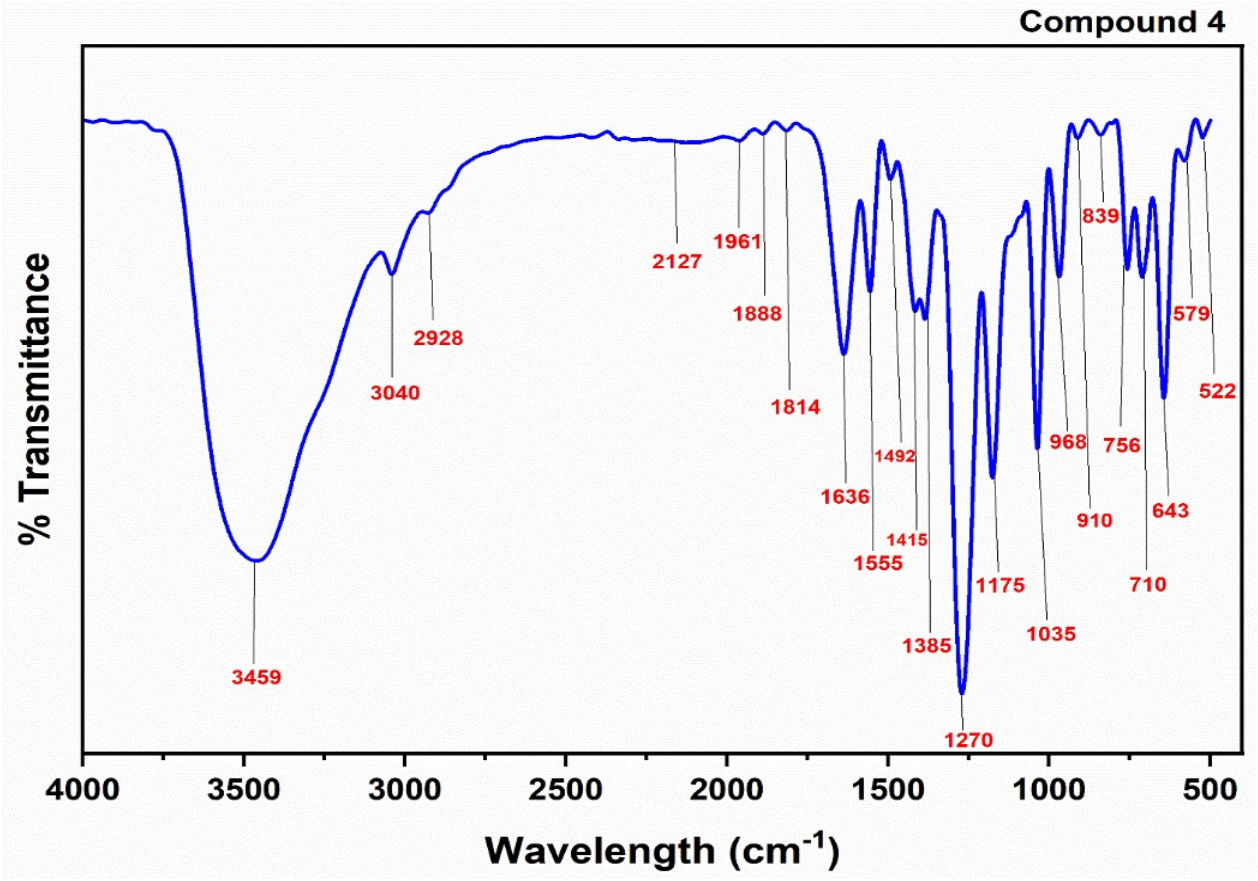

Fig. S28: FT-IR (KBr, cm^{-1}) spectrum of **4**.

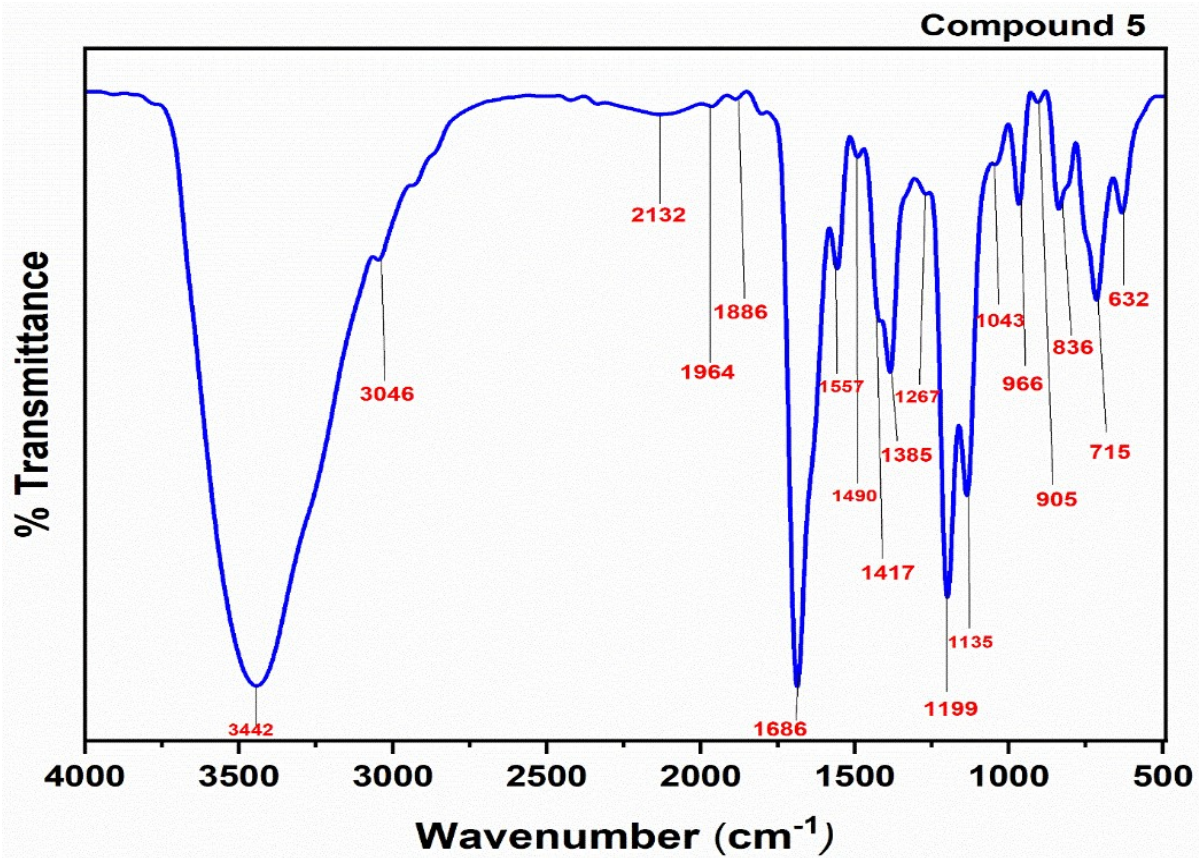

Fig. S29: FT-IR (KBr, cm^{-1}) spectrum of **5**.

5. UV-Vis absorption spectroscopy

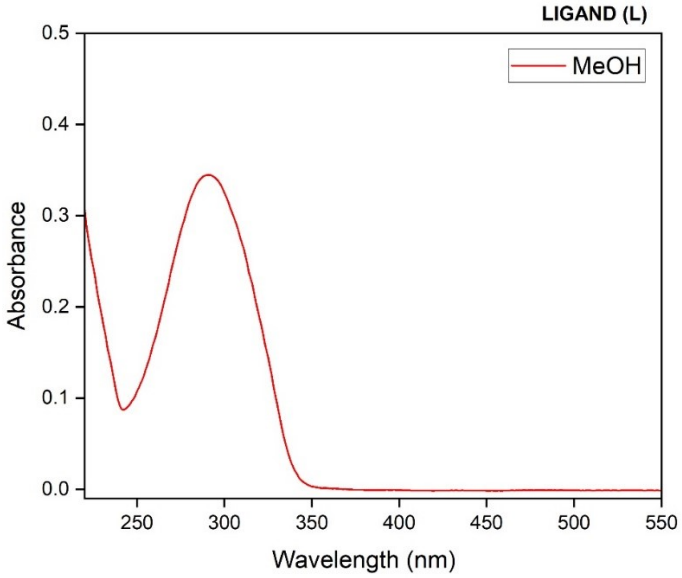

Fig. S30: UV spectrum of *trans*-5-Spym.

6. Analyses of Hirshfeld surfaces

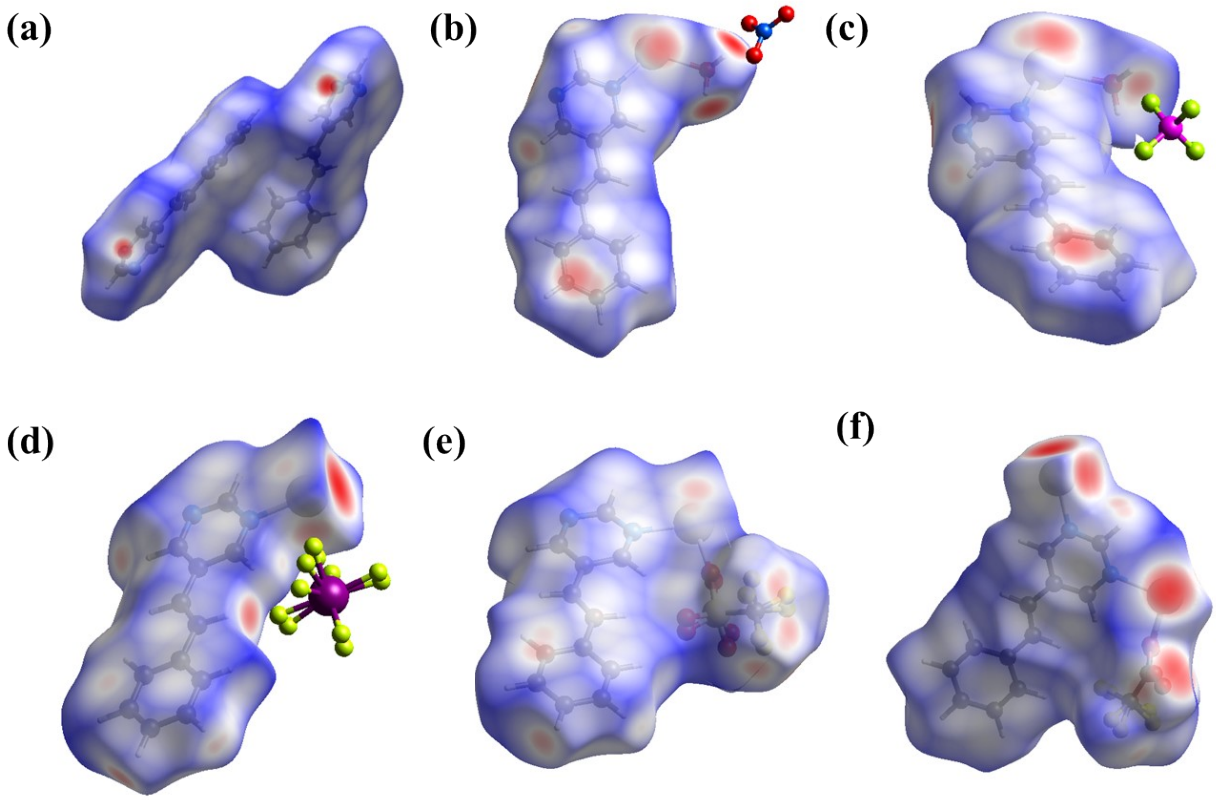

Fig. S31: Additional images of Hirshfeld surfaces mapped for d_{norm} for 5-Spym (a), and **1 – 5** (b-f).

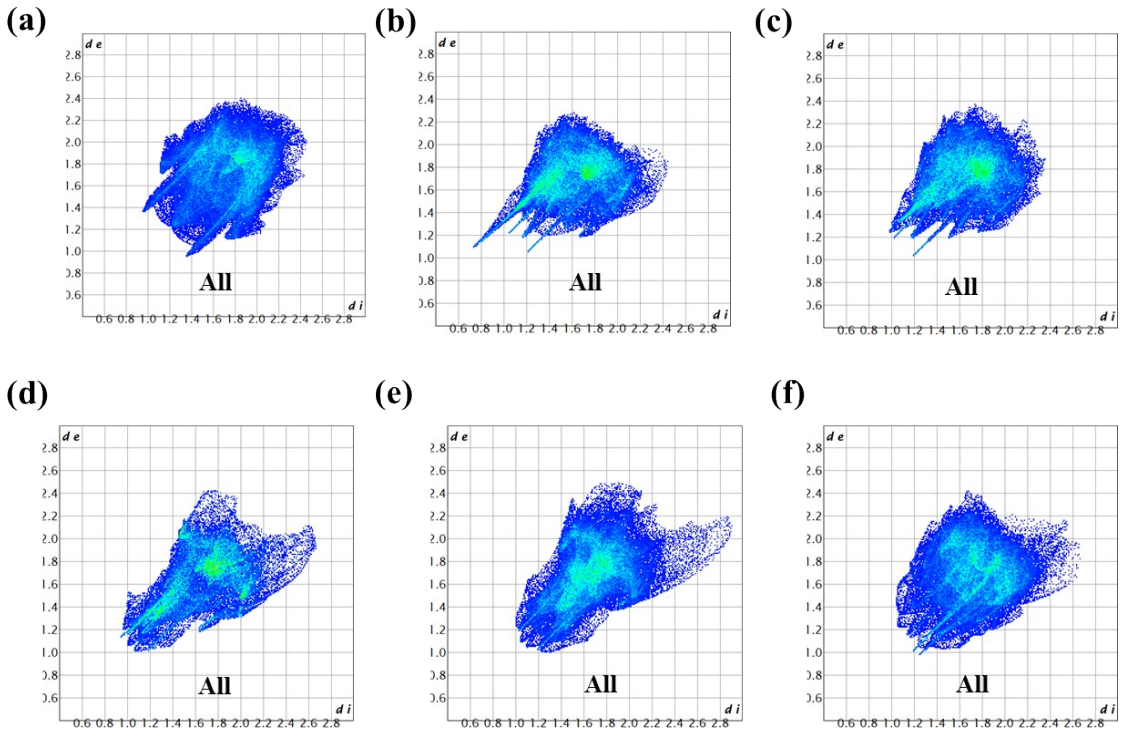

Fig. S32: Full 2D fingerprint plots for 5-Spym (a) and **1 – 5** (b – f).

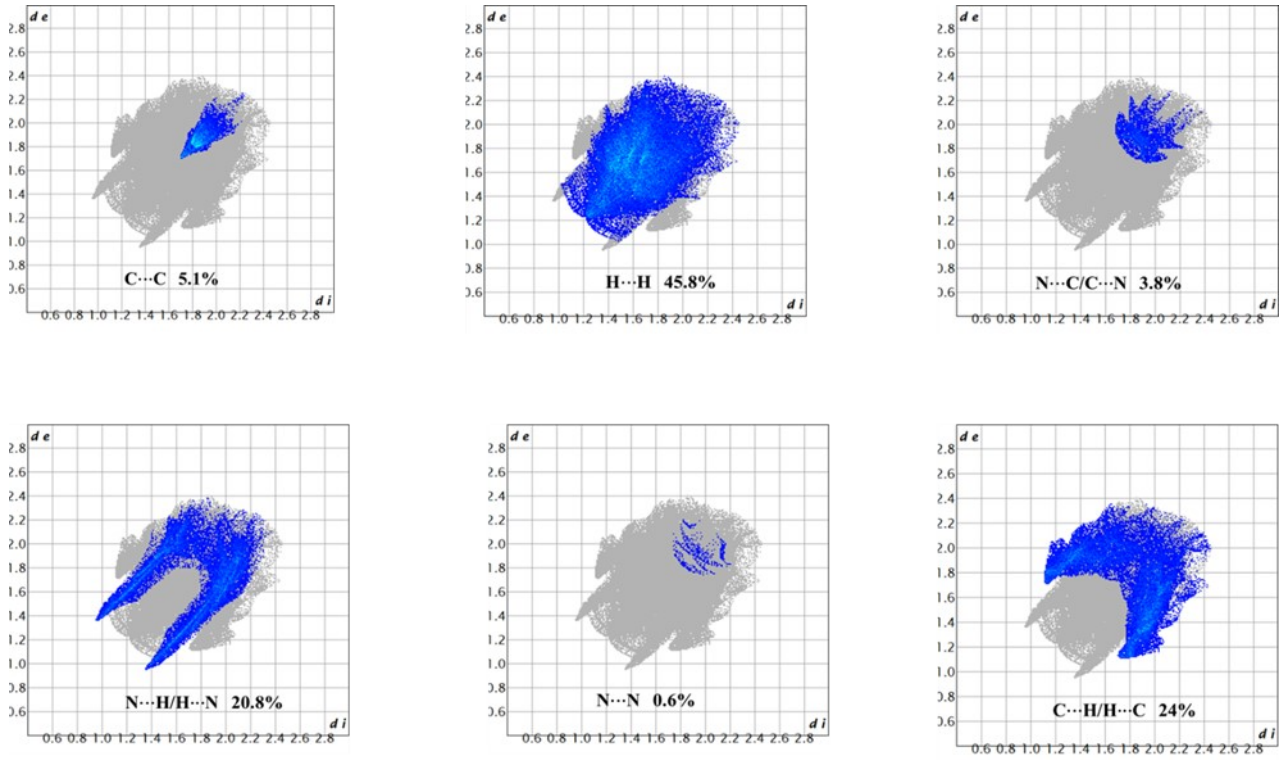

Fig. S33: Full fingerprint plot is resolved for various types of interactions and the percentage of their contributions to the total Hirshfeld surface area are presented for 5-Spym.

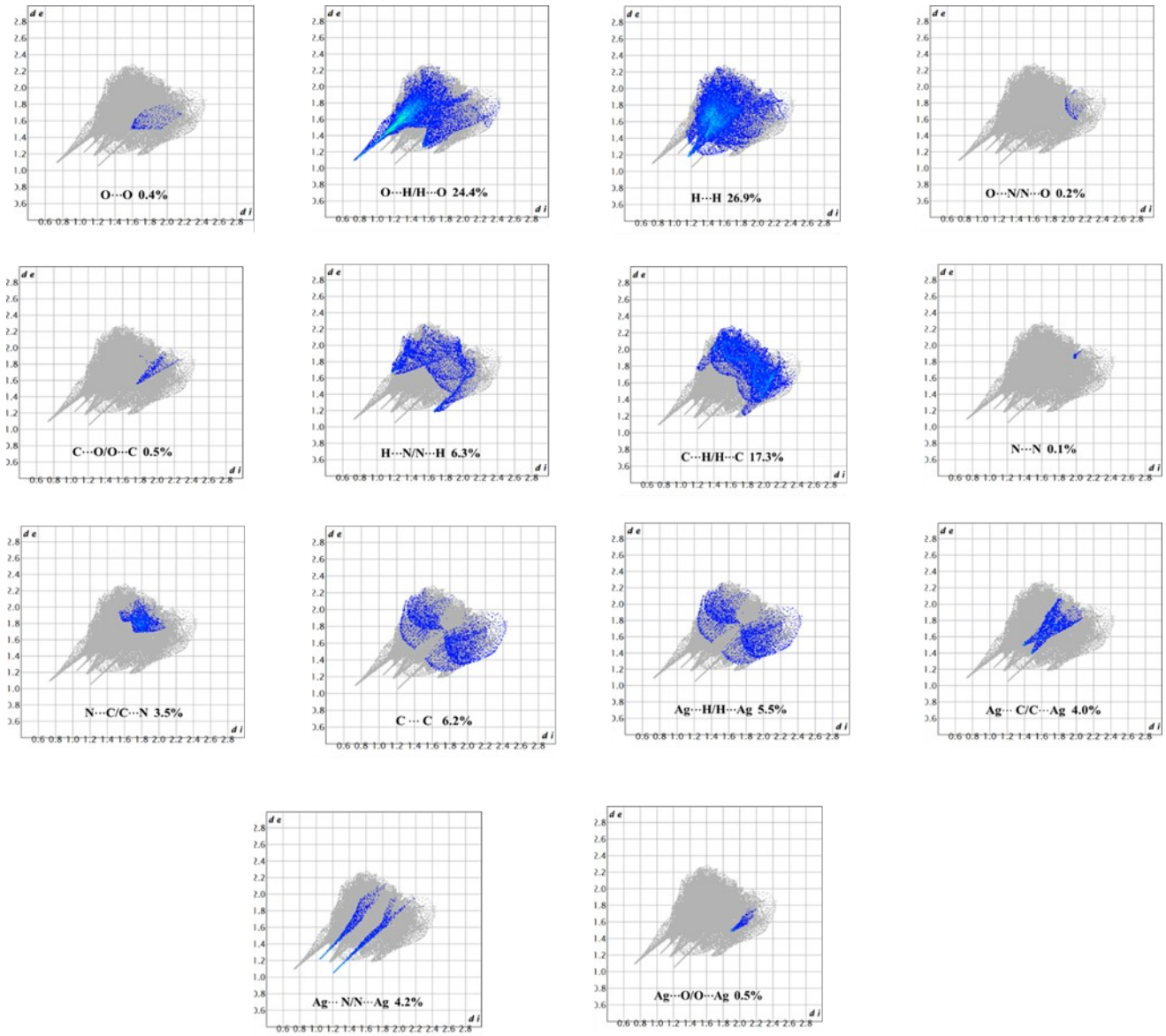

Fig. S34: Full fingerprint plot is resolved for various types of interactions and the percentage of their contributions to the total Hirshfeld surface area are presented for **1**.

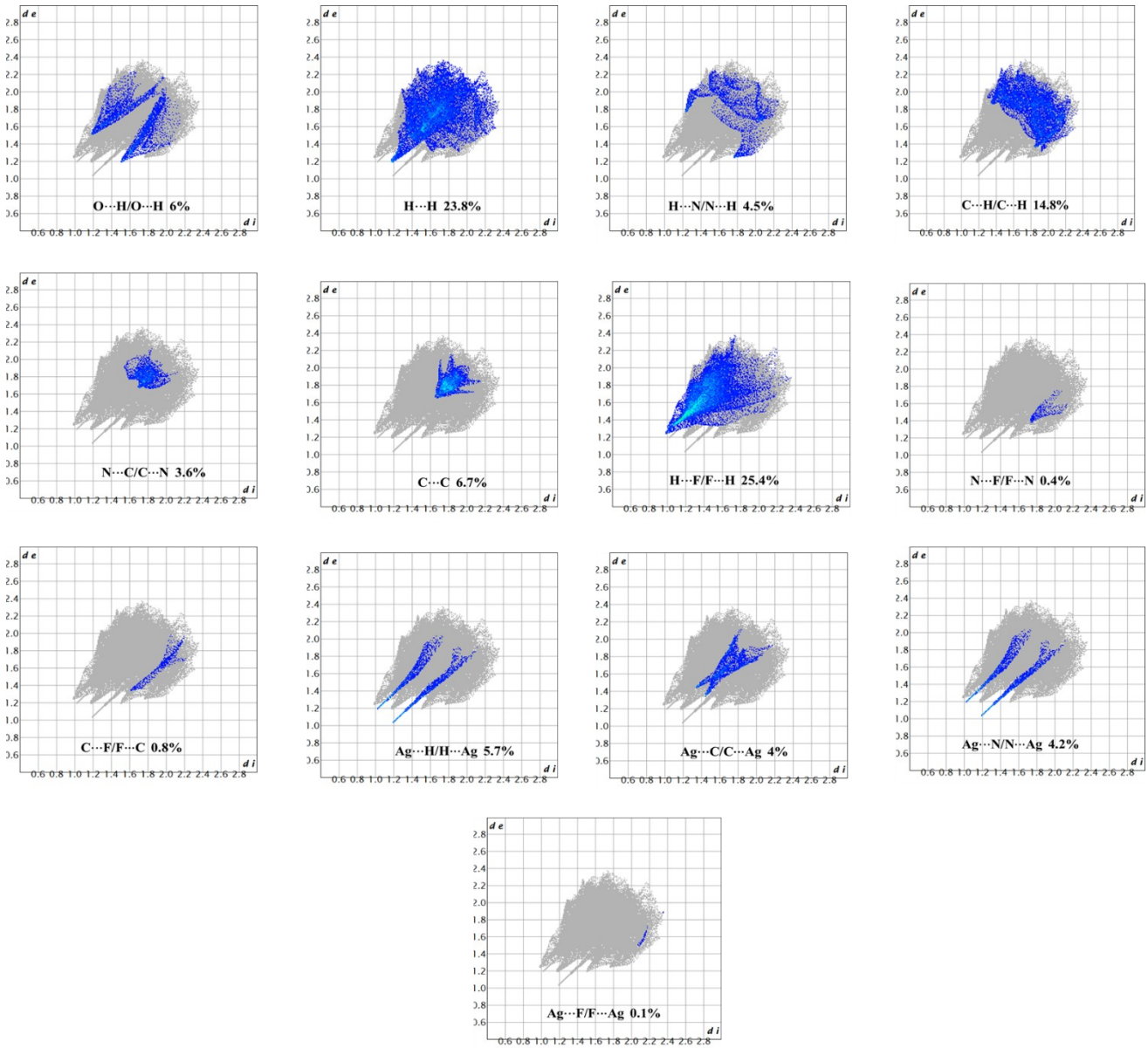

Fig. S35: Full fingerprint plot is resolved for various types of interactions and the percentage of their contributions to the total Hirshfeld surface area are presented for **2**.

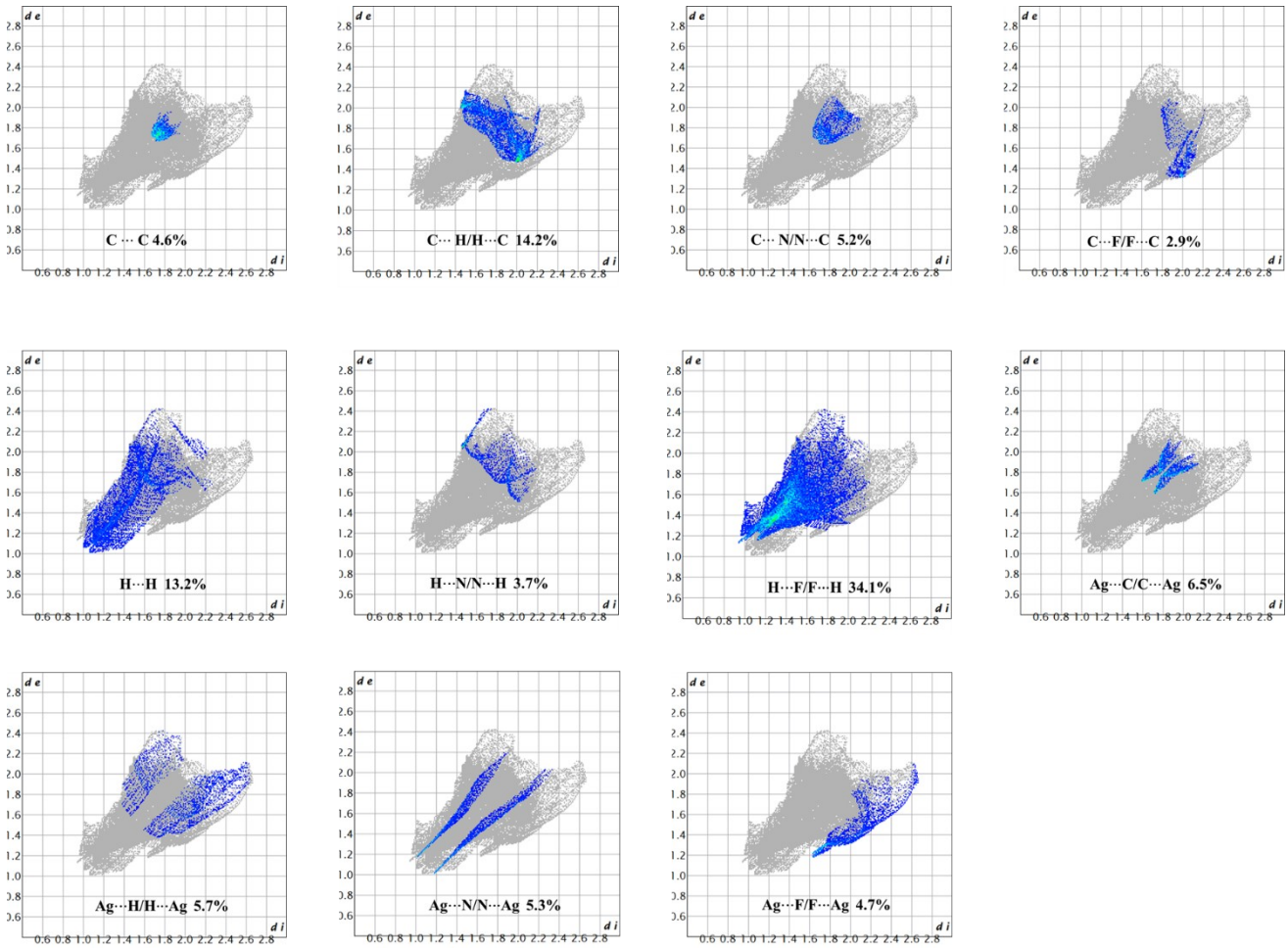

Fig. S36: Full fingerprint plot is resolved for various types of interactions and the percentage of their contributions to the total Hirshfeld surface area are presented for **3**.

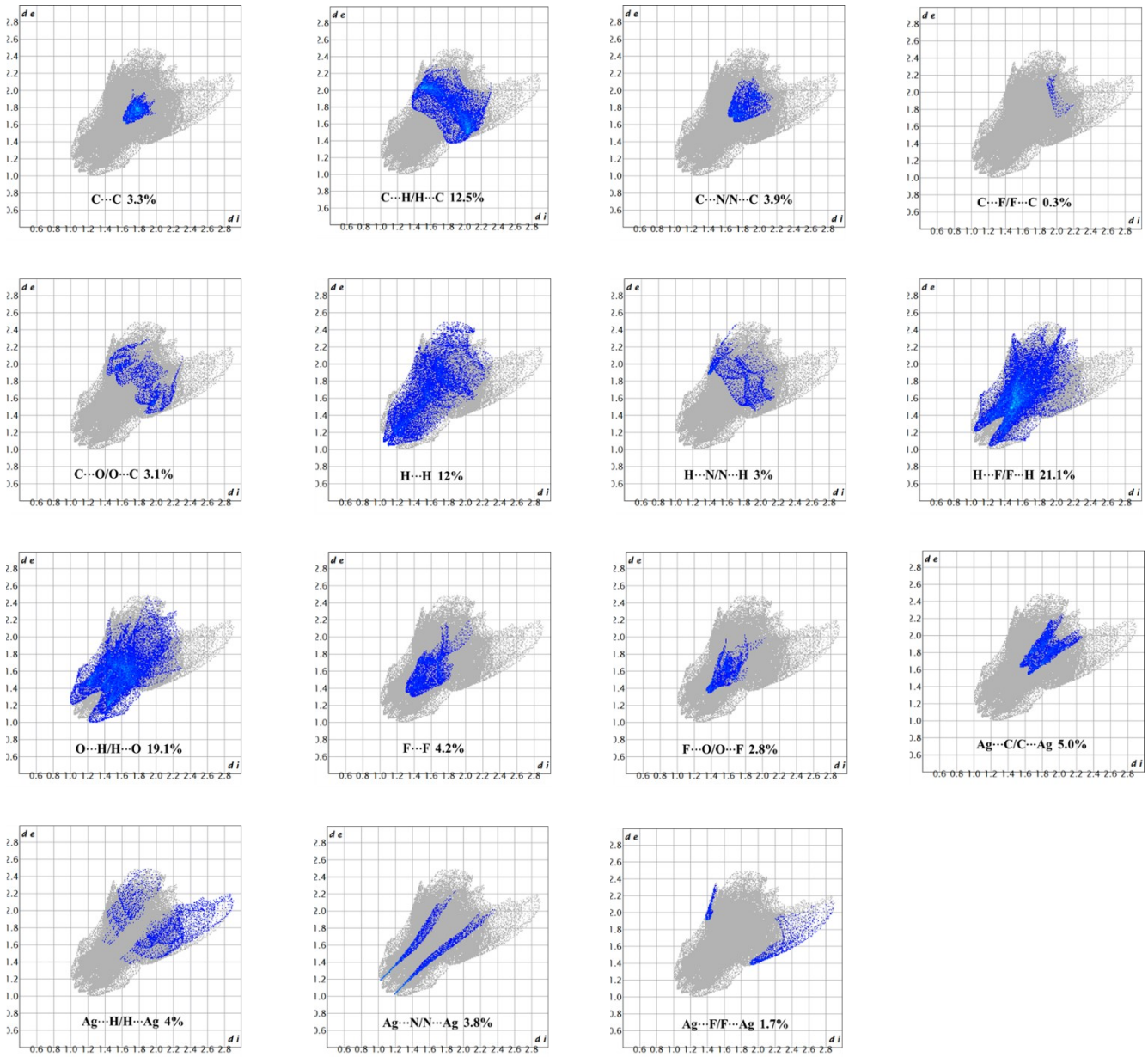

Fig. S37: Full fingerprint plot is resolved for various types of interactions and the percentage of their contributions to the total Hirshfeld surface area are presented for **4**.

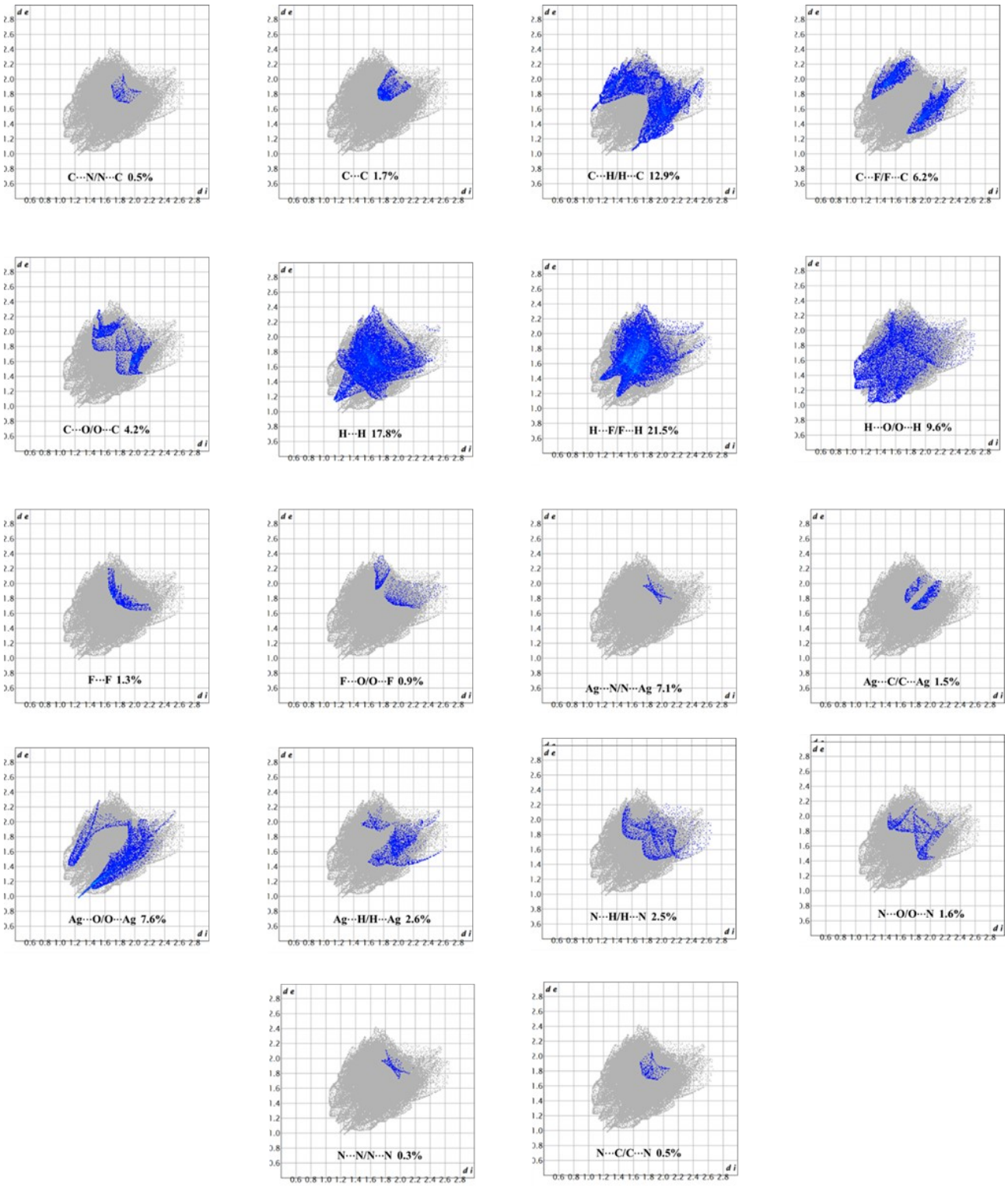

Fig. S38: Full fingerprint plot is resolved for various types of interactions and the percentage of their contributions to the total Hirshfeld surface area are presented for **5**.